



UNIVERSITÀ DEGLI STUDI DI SALERNO



UNIVERSITÀ DEGLI STUDI DI SALERNO

Dipartimento di Farmacia

PhD Program

in **Drug Discovery and Development**

XXX Cycle — Academic Year 2017/2018

PhD Thesis in

***Molecular basis of
cardiomiopathy***

Candidate Supervisor

Michela Pecoraro

Prof. *Ada Popolo*

Co-Tutor

Prof. *Aldo Pinto*

PhD Program Coordinator: Prof. Dr. *Gianluca Sbardella*

*I should apologize to my
self for believing I was not
enough*

ABSTRACT

The normal heart rhythm is guaranteed by an important intercellular junctions system, named Gap Junction (GJs). Each GJs consists of two units called connexons formed by six specific trans-membrane proteins named connexins (Cx). Recent reports suggest the presence of Cx43 in the inner mitochondrial membrane where it plays an important cardioprotection mechanism. Alterations in Cx43 expression and distribution were observed in several myocardium disease; i.e. in hypertrophic cardiomyopathy, heart failure and ischemia. Thus, in this doctoral study, we investigated the role of Cx43, and in particular of mitochondrial Cx43, in different cardiomyopathies models.

At first, we have investigated the involvement of mitochondrial Cx43 in an *in vitro* model of chemical hypoxia. Hypoxia was induced by adding Cobalt Chloride (CoCl₂) on H9c2 cardiomyoblast cell line, both in absence and in presence of Radicol, an Hsp 90 inhibitor that blocks Cx43 translocation to the mitochondria. Our results showed that CoCl₂ reduces the expression of Cx43 on the cell membrane and, moreover, it increases Cx43 expression at mitochondrial level, where it is involved in the regulation of reactive oxygen species production,

calcium storage and mitochondrial membrane depolarization. Furthermore, in an *in vivo* Doxorubicin (DOXO)-induced cardiotoxicity in a short-term mouse model we have studied the modulation of Cx43 expression/activity and its dysregulation. Our results showed that DOXO is able to induce significant changes in calcium homeostasis and alterations in Cx43 expression and localization. These effects are evident even in the heart of mice that received a single DOXO-administration. Finally, we have investigated if the pretreatment with Diazoxide (DZX), an opener of mitochondrial K_{ATP} -channels, attenuates DOXO-induced cardiotoxicity in a short-term mouse model. Our results demonstrate that DZX represents a promising protective intervention against DOXO-induced cardiotoxicity, by reducing the calcium homeostasis alteration and trying to restore the major cardiac parameters altered by DOXO treatment. This is in agreement with our hypothesis that mitochondrial Cx43 and DZX are involved in the cardioprotection mechanism.

Index

LIST OF ABBREVIATIONS	1
INTRODUCTION	3
AIM OF WORK	17
CHAPTER I: Role of mitochondrial Connexin 43 in a chemical model of hypoxia	19
1.1 Introduction.....	19
1.2 Material and Methods.....	21
1.2.1 Experimental Protocols	21
1.2.2 Cell Culture	21
1.2.3 MTT assay	22
1.2.4 Mitochondrial protein extraction and Western blot analysis for mitochondrial Cx43	23
1.2.5 Total protein extraction and Western blot analysis for procaspase 3 and caspase 9.....	24
1.2.6 Immunofluorescence Analysis with Confocal Microscopy.....	25
1.2.7 Measurement of Intracellular calcium Signaling.....	26
1.2.8 Measurement of Mitochondrial Superoxide Evaluation with MitoSOX Red	27
1.2.9 Measurement Mitochondrial Membrane Depolarization with TMRE.....	28
1.2.10 Cytochrome c release detection by cytofluorometry	29
1.2.11 Analysis of apoptosis.....	29
1.2.12 Statistical Analysis	30

1.3 Results	31
1.3.1 CoCl ₂ -induced chemical hypoxia	31
1.3.2 CoCl ₂ increased mitochondrial Cx43 expression	33
1.3.3 The inhibition of Cx43 translocation on mitochondria increased Mitochondrial Superoxide Production.....	35
1.3.4 CoCl ₂ induces calcium homeostasis alteration	36
1.3.5 The inhibition of Cx43 Translocation Enhanced Mitochondrial Membrane Depolarization	38
1.3.6 Inhibition of Cx43 translocation to mitochondria enhances CoCl ₂ -induced apoptotic response	39
1.4 Discussion	41

**CHAPTER II: Involvement of Connexin 43 in Calcium
Impairment induced by Doxorubicin
in a short-term mouse model..... 45**

2.1 Introduction	45
2.2 Materials and Methods	49
2.2.1 Materials	49
2.2.2 Animals.....	49
2.2.3 Experimental Protocols.....	49
2.2.4 Echocardiogram.....	51
2.2.5 Histological staining	51
2.2.6 Protein Extraction and Western Blot Analysis	51
2.2.7 Mitochondrial Protein Extraction and Western Blot Analysis for Mitochondrial Cx43 and pCx43	52
2.2.8 Primary Cardiomyocytes Isolation and Measurement of Intracellular Ca ²⁺ Signaling	53
2.2.9 Immunohistochemical Analysis.....	55
2.2.10 Statistical Analysis.....	55

2.3 Results	56
2.3.1 Cardiac Functions.....	56
2.3.2 Histopathological examination.....	57
2.3.3 Doxorubicin Administration Alters Calcium Homeostasis	58
2.3.4 Doxorubicin Administration Affects Cx43 Expression and Localization	61
2.4 Discussion.....	65

**CHAPTER III: Cardioprotective effects of
Diazoxide in Doxorubicin- induced
cardiotoxicity model69**

3.1 Introduction.....	69
3.2 Materials and Methods.....	73
3.2.1 Materials.....	73
3.2.2 Animals	73
3.2.3 Experimental Protocols	75
3.2.4 Echocardiogram.....	75
3.2.5 Protein Extraction and Western Blot Analysis	76
3.2.6 Mitochondrial Protein Extraction and Western Blot Analysis for Mitochondrial Cx43 and pCx43	77
3.2.7 Primary Cardiomyocytes Isolation and Measurement of Intracellular Ca ²⁺ Signaling.....	77
3.2.8 Immunohistochemical Analysis	79
3.2.9 Statistical Analysis	79
3.3 Results.....	80
3.3.1 Cardiac Functions.....	80
3.3.2 Diazoxide Administration Alters Calcium Homeostasis.....	81

3.3.3 Diazoxide Administration Affects Cx43 and pCx43 expression and localization.....	84
3.3.4 Diazoxide Administration Affects mitochondrial Cx43 and pCx43 expression.....	85
3.4 Discussion	88
GENERAL CONCLUSION	93
REFERENCES	95
PUBLICATIONS.....	121

LIST OF ABBREVIATIONS

Cx43	Connexin 43
GJ	Gap Junction
HSP90	Heat Shock Protein 90
mCx43	Mitochondrial Connexin43
mpCx43	Mitochondrial Connexin 43 phosphorylated
pCx43	Connexin 43 phosphorylated
PLB	Phospholamban
TMRE	Tetramethylrhodamina ethyl ester
TOM 20	Translocase of the Outer Membrane

INTRODUCTION

The steady beat of our hearts is among the most critical functions performed perfectly by our body without the conscious intervention. The developing heart is the earliest organ to function in the embryo, generating rhythmic contractions while it is forming, before there is blood to pump. Although the heart is composed of multiple cell types besides muscle cells, keeping a steady heartbeat is the job of specialized cardiomyocytes that ensure coordination of electrical signals throughout the organ [Rosenthal N.N et al., 2017].

Cardiac conduction has classically been viewed as an electrotonic process occurring by means of direct ionic current flow from cell to cell via Gap Junctions (GJs) [Kleber et al., 2004]. GJs are intracellular structures that provide connections and communication between cells, allowing the passage of ions and small molecules such as ATP, glutathione, cAMP, IP₃ and glucose [Pecoraro et al., 2015 a]. To form a GJ, six trans-membrane monomers (connexins) from one cell oligomerize to form a trans-membrane channel referred to as a connexon or hemichannel. The connexons from one cell then dock and couple with apposing connexons on neighboring cells and coalesce into dense GJ plaque [Basheer et al., 2016]. Connexins

are ubiquitous trans-membrane proteins and they are encoded by over 20 different genes in the mouse genome and 21 in the human genome, which are classified according to their different molecular weights that range between 26 and 60 kDa [Pecoraro et al., 2015 a]. Each connexin is constituted by four trans-membrane domains, two extracellular loops (EL) and one intracellular; amino and carboxy terminal regions are both located in the cytosol [Solan and Lampe, 2005].

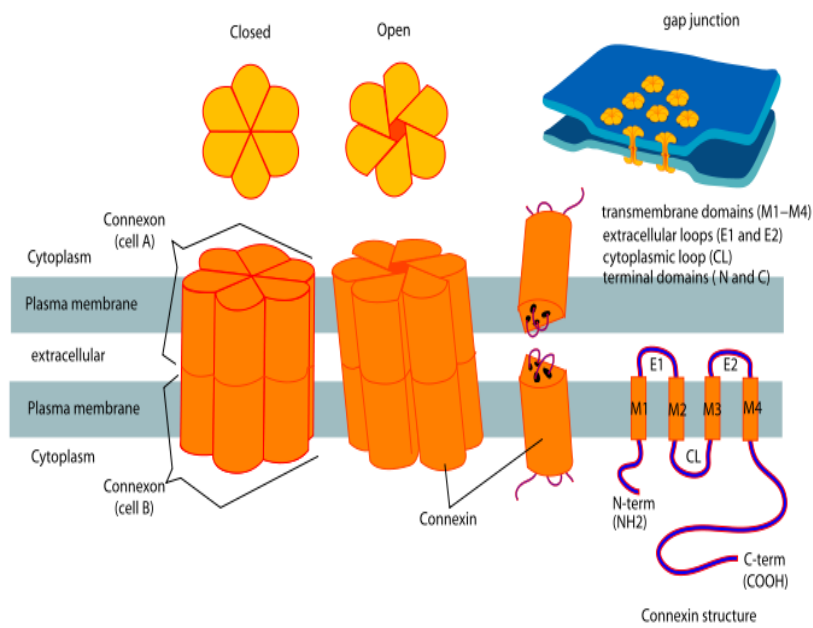


Figure 1: The image shows a GJ and its main element.[LadyofHats et al., 2006]

Connexin 43 (Cx43) is the major connexin expressed in the cardiac ventricle, [Willecke et al., 2002; Pecoraro et al., 2017 a], which regulate intercellular coupling, conduction velocity, and anisotropy [Cabo et al., 2009]. It is also responsible for the action potential propagation [Severs et al., 2008] and it

critically regulate intercellular translocation of ions and small molecules [Van Veen et al., 2001]. Indeed, many reports have suggested that Cx43 regulates other cellular mechanisms, including the cell cycle, differentiation, proliferation [Kardami et al., 2007], maintenance of tissue homeostasis, and embryogenesis [De Maio et al., 2002].

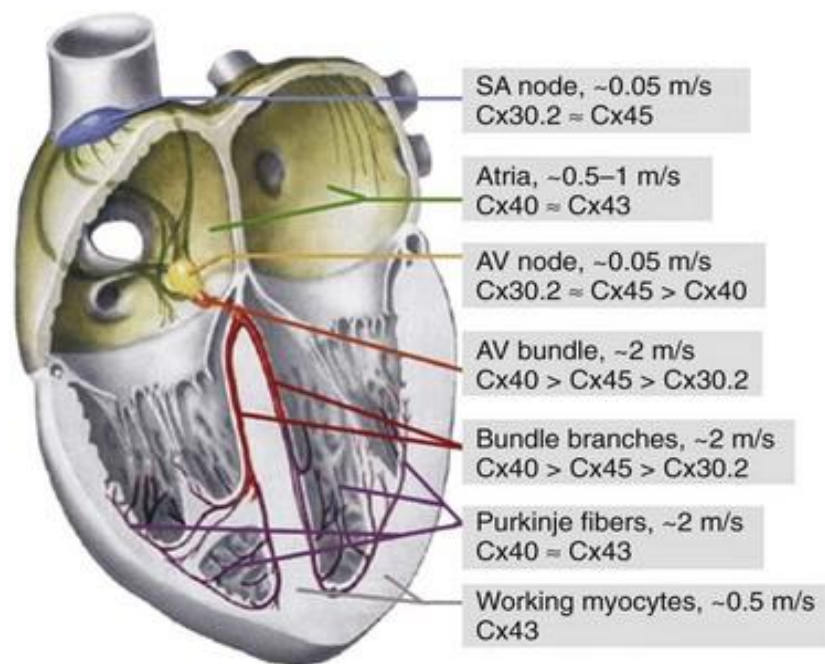


Figure 2: Molecular Organization, Gating, and Function of Gap Junction Channels [Feliksas et al., 2013]

Cx43 has a short half-life (1–3 hours in the myocardium) [Beardslee et al., 1998; Smyth et al., 2014]. It oligomerizes in the Golgi/trans-Golgi network and, after assembly, it is transported to the non-junctional plasma membrane through the cytoskeleton. Once inserted into the cell membrane, Cx43 spreads in the region where there are GJ plaques by a

microtubule/dynein/ β -catenin/N-cadherin-dependent pathway [Sáeza et al., 2010].

In the heart, localization of Cx43 at the intercalated discs is crucial to provide the intercellular coupling necessary for rapid action potential propagation through the myocardium and synchronized cardiac contraction [Rohr et al., 2004].

Cx43 hemichannels can occur as free, non-junctional channels in the plasma membrane. These hemichannels are normally closed but may open in response to various triggers including cell depolarization, decreased extracellular Ca^{2+} ion concentration, increased intracellular Ca^{2+} concentration and alterations in the phosphorylation or redox status [Basheer et al., 2016]. Generally, it has been assumed that the opening of plasma membrane Cx43 hemichannels is linked to pathological rather than physiological entities, contributing to cell swelling and cell death. In the cardiac cells, excessive hemichannel opening allows the entry of Na^+ and Ca^{2+} and the escape of K^+ , adenosine triphosphate (ATP) and other small metabolites, leading to osmotic shifts, energy depletion, Ca^{2+} overload and cell death promotion [Schulz et al., 2015]. Therefore, blockage of the Cx43 hemichannels by using pharmacological inhibitors can possibly have protective effects against cardiac insult such as in the case of ischemia/reperfusion injury [Schulz et al., 2015; Wang et al., 2013].

Mice lacking Cx43 die shortly after birth due to cardiac hyperplasia obstructing the right ventricular outflow tract [Reaume et al., 1995], while a heart-specific conditional knockout exhibited arrhythmia and premature death [Gutstein et al., 2001a; Gutstein et al., 2001 b].

Cx43 is a phosphoprotein that is predominantly phosphorylated in the control state. There are at least 14 serines and 2 tyrosines in the cytoplasmic C-terminal region of Cx43 that are phosphorylated by a variety of kinases [Marquez-Rosado et al., 2011], such as mitogen activated protein kinase (MAPk), protein kinase C (PKC), protein kinase A (PKA), casein kinase 1 and Src. The phosphorylation of the serine residues, like S306, S365 and S368, modulates the conductivity of the GJs [Lampe et al., 2000], as well as their trafficking, assembly/disassembly, degradation and gating [Pecoraro et al., 2015 a]. Indeed, connexin phosphorylation and dephosphorylation play an important role in regulating GJ channel function at several stages of the cell cycle and the connexin “life cycle” [Hood et al., 2017].

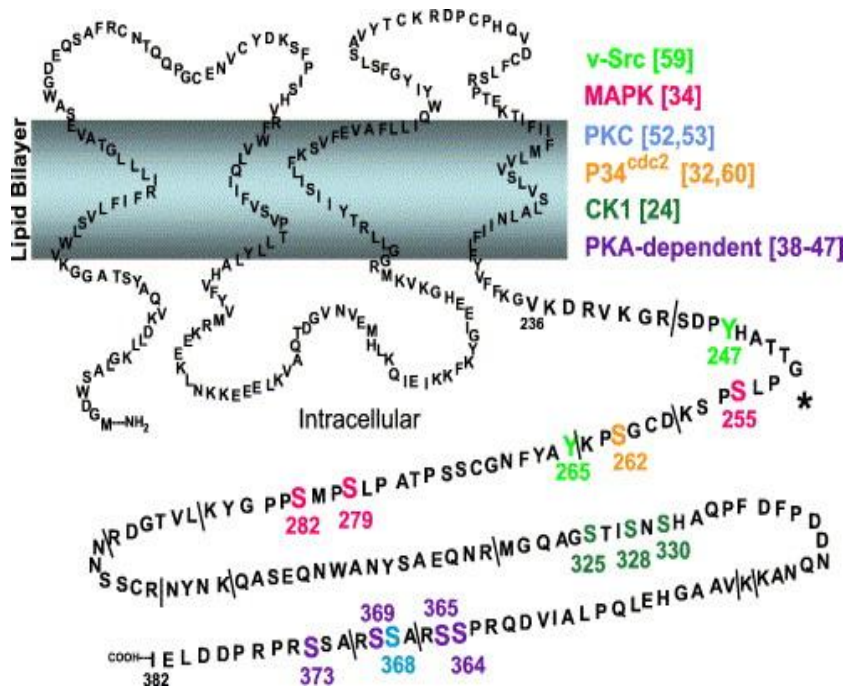


Figure 3: Connexin phosphorylation at the serine residues modulates the conductivity of the GJs, as well as, their trafficking, assembly/disassembly, degradation and gating [Solan and Lampe 2005]

Most of the function ascribed to Cx43 in cardiac pathophysiology is within the context of its role in forming the GJ [Severs et al., 2004]. However, recent literature reports that Cx43, independent of its ability to form functional GJs, regulates susceptibility of cells to several cell injury paradigms suggesting a novel function of this protein in modulating cell death, specially myocyte death [Li et al., 2003].

Cardiac mitochondria play a pivotal role in the maintenance of cellular bioenergetics and intracellular ion homeostasis, especially of calcium (Ca^{2+}) and potassium (K^+) ions. Cellular Ca^{2+} homeostasis is maintained in a very stringent manner by the cyclical uptake and release by the endoplasmic reticulum

and mitochondria, respectively [Gunter et al., 2004]. These cyclical events are crucial to ensure the cardiac rhythm and any disturbance may lead to arrhythmia, cell death, and tissue damage as observed in cardiac failure and ischemia–reperfusion injury [Kristia´n et al., 1998]. Many studies reported that both in tissue [Boengler et al., 2005; Pecoraro et al., 2017 b] and in isolated mitochondria [Srisakuldee et al., 2009; Pecoraro et al., 2017 b], Cx43 is located at the inner mitochondrial membrane [Rodriguez-Sinovas et al., 2006] where it forms hemichannels, with the C-terminus region oriented at the intermembrane space [Miro-Casas et al., 2007].

The physiological role of mCx43 has not been well elucidated, but recent studies show that it modulates K^+ influx to the mitochondrial matrix, mitochondrial respiration and reactive oxygen species (ROS) generation [Boengler et al., 2012; Miro-Casas et al., 2007]. Indeed, mCx43 may play a role in mediating the cardioprotective effect of ischemic preconditioning. Protection by mCx43 has been linked to ROS generation, mitochondrial K_{ATP} channels, protein kinase C (PKC) signaling, and stimulation of translocase of outer membrane- 20 (Tom20) that facilitates Cx43 transport [Gadicherla et al., 2017], from cytosol to mitochondria with a mechanism that involves heat shock protein 90 (Hsp90). Cytosolic Hsp90 is generally involved in the folding of newly synthesized proteins and its

role in mitochondrial import may be an extension of this activity [Young et al., 2003].

In fact, mitochondrial import machinery involves binding of the target protein to a chaperone (Hsp90/Hsp70), presentation to specific parts of TOM complex, and release into the inner mitochondrial membrane through the TIM (Translocase of the Inner Membrane) [Pecoraro et al., 2015 a]. Recently it has been hypothesized that mCx43 protects the cells by reducing cytosolic Ca^{2+} overload, mitochondrial permeability transition, and cell death [Pecoraro et al., 2017 a; Pecoraro et al., 2017 b]. Cx43-based hemichannels are non-selective large conductors of Ca^{2+} entry in the inner mitochondrial membrane. Thus, mCx43 may directly contribute to mitochondrial Ca^{2+} entry/overload, permeability and cell death [Wang et al., 2013; Decrock et al., 2011].

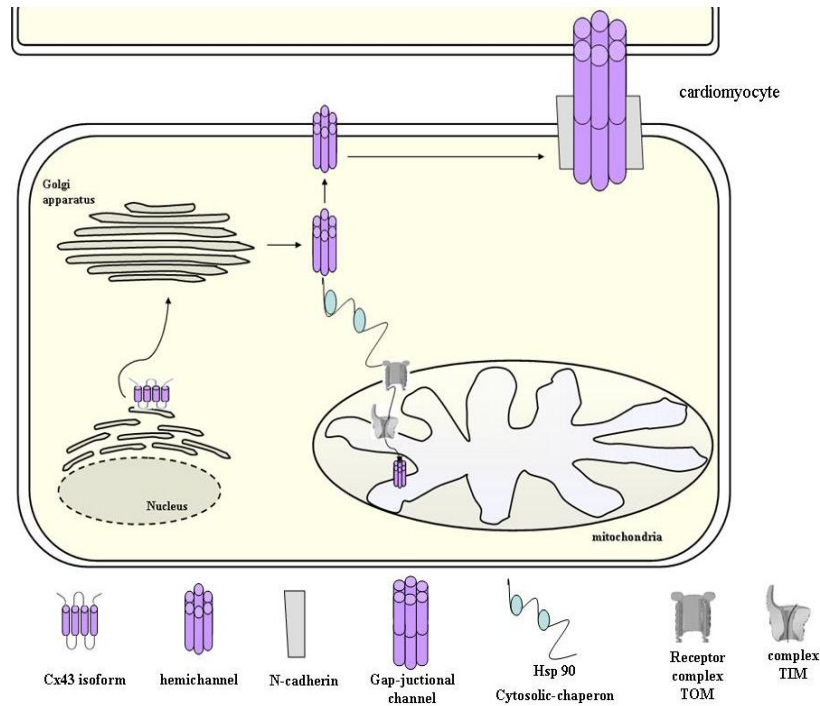


Figure 4: During biosynthesis, Cx43 is inserted into the endoplasmic reticulum where it correctly folds and oligomerize in the Golgi/trans-Golgi network. After assembly, Cx43 hemichannel is carried on the cell surface through the cytoskeleton. Once inserted into the cell membrane, Cx43 spreads in the region where there are GJ claque by a microtubule/dynein/ β -catenin/N-cadherin-dependent pathway. In addition, after assembly in Golgi, Cx43 may translocate from cytosol to mitochondria with a mechanism that involves Hsp90 and translocase of the outer membrane. This system involves binding of the target protein to Hsp90, presentation to specific parts of TOM complex, and release into the inner mitochondrial membrane [Pecoraro et al., 2015 a].

Myocyte apoptosis is now recognized to mediate cell death in a variety of acute and chronic heart diseases [Goubaeva et al., 2007], and many studies confirmed the mCx43 as a novel regulator of mitochondrial function where inhibition results in the release of cytochrome C and myocyte apoptosis.

Futhermore, mCx43 is involved in a signal transduction pathway that can prevent mitochondrial permeability transition pore (mPTP) formation [Ruiz-Meana et al., 2008]. The mPTP is a large non-specific conductance channel that forms at the inner mitochondrial membrane under conditions of calcium

overload/oxidative stress [Baines et al., 2007]. Once formed the mPTP results in mitochondrial swelling, rupture of the outer mitochondrial membrane, release of apoptogenic mitochondrial contents to the cytosol, and cell death. Signals preventing mPTP formation during reperfusion after ischaemia promote cell survival and reduce myocardial damage [Martel et al., 2012].

Thus, Cx43 channels, both as a GJ and as a hemichannel, form large-conductance ion channel with chemical gating similar to the Bcl-2 channels. In addition, they are voltage gated perhaps allowing sensing of the mitochondrial membrane potential in addition to the chemical environment.

Changes in Cx43 expression and/or subcellular distribution in the heart have been associated with a wide variety of pathologic conditions and diseases, including the ventricular myocardium and cardiac arrhythmia [Due t al., 2017; Prevedel et al., 2017]. Moreover, myocardial hypoxia or ischaemia and conditions such as hypertrophy are associated with reduced cardiac action potential conduction, raised intracellular $[Ca^{2+}]$ and GJ uncoupling [Jabr et al., 2016].

These alterations contribute to abnormal impulse propagation and arrhythmogenic substrates leading to sudden cardiac death [Gutstein et al., 2001]. Arrhythmias are common complications of myocardial ischemia and infarction in humans. Reduced electrical coupling can increase the propensity for arrhythmias

rendering the ventricle more susceptible to re-entry. This condition seems to be due to dysfunction and disorganization of Cx43. Indeed, reduction of about 90% in Cx43 expression results in about 50% decrease in the conduction velocity. While 50% reduction in Cx43 may lead to some conduction slowing, high levels of electrical uncoupling are needed to increase arrhythmogeneity [Pecoraro et al., 2015 a].

Therefore, a large number of studies in recent years demonstrated a decrease in expression and/or lateralization and heterogeneous distribution of Cx43 in the myocardium of patients with hypertrophic cardiomyopathies (HCM), dilated cardiomyopathies (DCM), ischemic cardiomyopathies, as well as clinical congestive heart failure [Basheer et al., 2016].

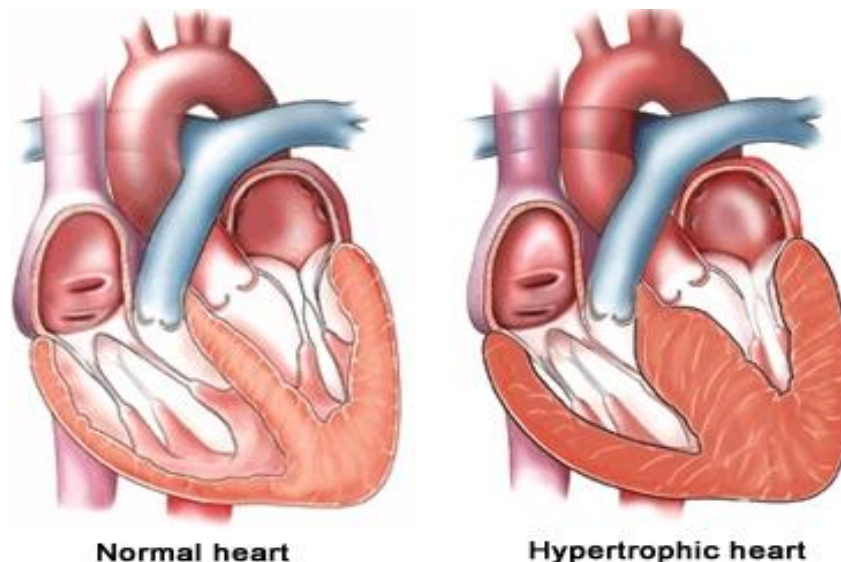


Figure 5: Hypertrophic Cardiomyopathy and Heart Failure. Hypertrophy are associated with reduced cardiac action potential conduction, raised intracellular $[Ca^{2+}]$ and GJ uncoupling [Columbia University]

In general, in these cardiomyopathies, Cx43 expression appears to be unaltered or up-regulated during the initial and compensatory phase of hypertrophy, but redistributed along the cardiomyocyte surface and reduced when the hypertrophy becomes prolonged and putatively maladaptive in its progression to heart failure [Birgit et al., 2004].

The most common myocardial dysfunction is ischemic injury, which is the principal cause of death in the world [Pecoraro et al., 2017 a].

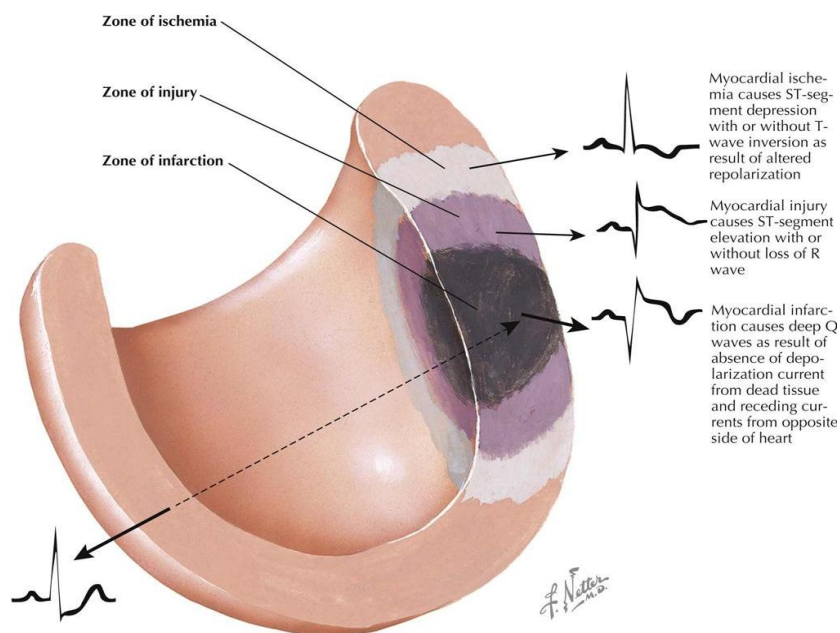


Figure 6: Ischemic injury, the principal cause of death in the world. [Netter F et al., 2015]

Cardiac ischemia is manifested by accumulation of metabolites in the extracellular compartment in combination with reduced oxygen supply. Furthermore ischemia induces closure of GJs, due to increased cytosolic Ca^{2+} concentration, reduced ATP concentration, changes in phosphorylation of Cx43 and acidification [Johansen et al., 2011]. Increased levels of intracellular Ca^{2+} and H^+ and accumulation of amphipathic lipid metabolites during ischemia promote electrical uncoupling, mediated by alterations in phosphorylation of Cx43. In fact, acute ischemia may activate or inhibit protein kinases and phosphatases [Beardslee et al., 2000]. Cx43 plays a crucial role in ischemic preconditioning cardioprotection by improving myocardial function [Wang et al., 2015].

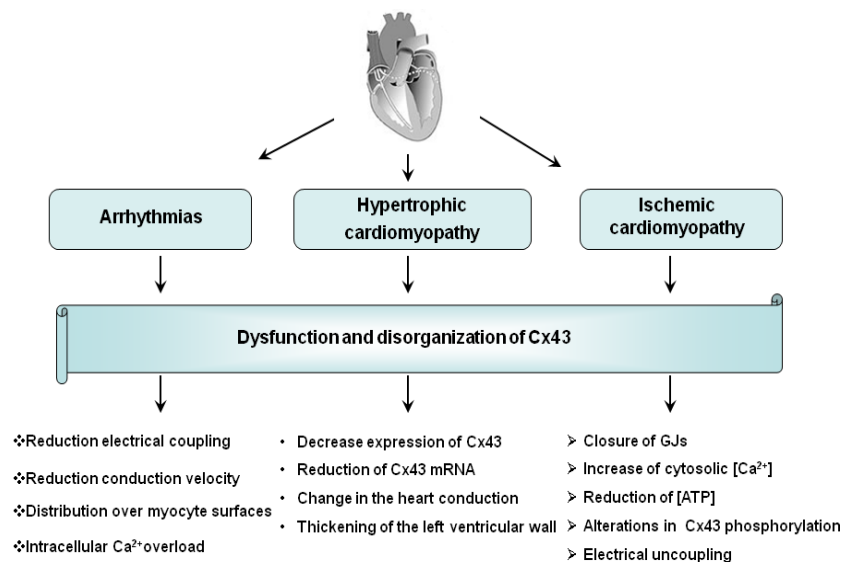


Figure 7: Schematic diagram that shows the effects of Cx43 dysfunction and disorganization in the main heart disease [Pecoraro et al., 2015 a]

AIM OF WORK

Based on the data recently reported in the literature [Pecoraro et al., 2015 b; Severs et al., 2004; Du et al., 2017], we hypothesized that GJs, particularly Cx43, are largely involved in mechanisms that affect different cardiac pathologies. The aim of this doctoral project is therefore to investigate the involvement of Cx43, and in particular of the mCx43, in *in vitro* and *in vivo* cardiomyopathies models. In addition, we will focus on specific drugs and on their effects on the modulation of Cx43 expression/activity.

-As the first we investigated the involvement of mCx43 in the apoptotic pathway in an *in vitro* model of chemical hypoxia. Hypoxia was induced by adding Cobalt Chloride (CoCl_2) on H9c2 cardiomyoblast cell line, both in absence and in presence of Radicicol, an Hsp 90 inhibitor that blocks Cx43 translocation to the mitochondria.

-As the second we investigated the involvement of Cx43 in a mouse model of cardiotoxicity. To this end we used a short-term mouse model of cardiotoxicity induced by Doxorubicin.

-As the third we investigated if the pretreatment with Diazoxide (DZX), an opener of mitochondrial K_{ATP} -channels, attenuates DOXO-induced cardiotoxicity and affect Cx43 expression and/or localization in a short-term mouse model.

Chapter I

Role of mitochondrial Connexin 43 in a chemical model of hypoxia

1.1 Introduction

Ischemic injury is the most common myocardial dysfunction, which is the principal cause of death in the world [Ruiz-Meana et al., 2001]. It's irreversible and widespread loss of myocardial cells and subsequent ventricular remodeling induced by acute myocardial infarction are the main elements resulting in chronic heart failure and permanent loss of labor force [Roger et al., 2012].

This cardiomyopathy is manifested by accumulation of metabolites in the extracellular compartment in combination with reduced oxygen supply [Pecoraro et al., 2015 a].

Ischemia triggers a decrease in GJ communication as a result of acidosis, increased intracellular Ca^{2+} concentration ($[\text{Ca}^{2+}]_i$) and altered phosphorylation and nitrosylation levels [Schulz et al., 2015]. Revascularization could improve the prognosis of the patients with acute myocardial infarction [Roger et al., 2012], however, reperfusion could induce additional injury, which is sometimes extremely severe or fatal. Basic studies [Jiang et al., 2013; Wei et al., 2013] and small-sample clinical data [Crimi et

al., 2013] have verified that ischemic postconditioning (IPOC) could attenuate injury induced by ischemia/reperfusion (I/R). Other studies [Shimizu et al., 2014; Mykytenko et al., 2008] report that the Cx43 plays an important role in IPOC cardioprotection against I/R injury. In fact, many studies attribute the effect of cardioprotection to mitochondria, where Cx43 translocates through Hsp90/TOM 20 machinery system [Goubeva et al., 2007].

So, the first step of this PhD project was to study the role of mCx43 in an *in vitro* model of hypoxia.

1.2 Materials and Methods

1.2.1 Experimental Protocols

The hypoxia model was established by using the hypoxia-inducing agent CoCl₂ [Shi Yun et al., 2017]. CoCl₂ is a well known chemical hypoxia mimetic agent, which can mimic hypoxia/hischemic conditions by causing inactivation of hydroxylase enzymes and stabilization of hypoxia-inducible factor HIF-1 α [Liu et al., 2014]. H9c2 cardiomyoblasts were treated with CoCl₂ at 50-100-150 μ M for 3 or 6 h in DMEM 10 % FBS. In order to verify the role of mCx43 in CoCl₂-treated cells, we used Radicicol, a specific inhibitor of Hsp90 [Schulte et al., 1998], since the translocation of mCx43 on the mitochondrial membrane provides the binding of this protein to Hsp90 [Ruiz-Meana et al., 2008]. In the experiments that included the use of Radicicol (1 μ M), an Hsp90 inhibitor, it has been administered 30 min before CoCl₂ treatment and left in the incubation medium for all experimental time.

1.2.2 Cell Culture

The cell line used is rat cardiomyocytes H9c2 that demonstrate many similarities to primary cardiomyocytes, including membrane morphology, G-protein signaling expression, electrophysiological properties and constitutive expression of

Cx43 [Wu et al., 2013]. H9c2 was purchased from the American Tissue Culture Collection (Manassas, VA, USA).

H9c2 cells were subcultured weekly in 100-mm Corning dishes containing 10 ml Dulbecco's modified Eagle's Medium (DMEM; Gibco) with 10 % fetal bovine serum (FBS; Gibco) and antibiotics (25 U/ml penicillin and 25 U/ml streptomycin).

1.2.3 MTT assays

Cell viability was evaluated by means of MTT ([3-(4,5-dimethylthiazol-2-yl)-2,5-diphenyltetrazolium bromide]). H9c2 ($3,5 \times 10^3$ cells/well) were plated in 96-well tissue culture plates and allowed to adhere for 24 h. Thereafter, the medium was replaced with fresh medium alone or containing CoCl_2 (50-100-150 μM) and incubation was performed for 3 or 6 h at 37°C in an atmosphere containing 5% CO_2 . Where indicated, Radicicol (1 μM) was added 30 min before CoCl_2 . Cell mortality was assessed by means of MTT assay. Briefly, 25 μl of MTT (5 mg/ml) were added and cells were incubated for an additional 3h to allow the formation of formazan precipitate, which was solubilised with 100 μl of a solution containing 50% (v/v) N,N-dimethylformamide, 20% (w/v) SDS with an adjusted pH of 4.5. The optical density (OD) of each well was measured with a microplate spectrophotometer (Titertek Multiskan MCC/340-DASIT; Milan, Italy) equipped with a 620nm filter. H9c2

mortality in response to treatment with CoCl_2 both in absence and in presence of Radicol was calculated as % mortality = $100 - [100 \times (\text{OD treated} / \text{OD control})]$.

1.2.4 Mitochondrial protein extraction and Western blot analysis for mitochondrial Cx43

H9c2 (1×10^6 cells/well) were seeded into Petri plates and allowed to adhere for 24 h. Thereafter, the medium was replaced with fresh medium and cells were treated as described. Mitochondrial protein extraction was carried out from cells in lysis buffer A (sucrose 250 mM, K^+ Hepes pH 7.5 20 mM, KCl 10 mM, MgCl_2 1,5 mM, EDTA 1 mM, EGTA 1 mM, protease inhibitors, NaF 50 mM, Na_3VO_4 0,2 mM, PMSF 1 mM, DTT 1 mM, digitonin 0,025%). Then the cells were centrifugated at 16000 g for 2 min at 4°C. The supernatant was discarded and the pellet was resuspended in lysis buffer B (NaCl 150mM, Triton X 1%, NaDeOH 0,5%, SDS 1% and Tris HCl 50mM pH 7.4) to obtain mitochondrial protein. Protein concentrations were determined with the Bio-Rad protein assay (BIO-RAD, Milan Italy). Equal amounts of protein (50 μg) were loaded into an acrylamide gel and separated by SDS-PAGE under denaturing conditions. Blots were incubated with primary antibody anti-Cx43 (BD transduction laboratories, 1:8000) or anti-TOM20 (1:250, used as loading control) over night. After incubation

with the primary antibodies and washing in PBS/0.1% Tween, the appropriate secondary antibody, anti-rabbit or anti-mouse (each diluted 1:4000) was added for 1h at room temperature. Immunoreactive protein bands were detected by chemiluminescence using enhanced chemiluminescence reagents (ECL) in LAS 4000 (GE Healthcare). The images were analysed for densitometry using ImageJ Software.

In order to verify the purity of mitochondrial protein extraction, a Western blot analysis was performed to evaluate the presence of proteins expressed only in the mitochondria (ox-Phos Complex II, Abcam, 1:7000) and the absence of proteins expressed in other cellular compartments (Na^+/K^+ ATP_{ase}, Abcam, 1:3000). The purification assay was evaluated as the enrichment in mitochondrial protein (anti-Ox-Phos Complex II) as well as the elimination of the other cellular constituent (anti- Na^+/K^+ ATP_{ase}) by means of Western blot analysis as previously reported [Boengler et al., 2005].

1.2.5 Total protein extraction and Western blot analysis for procaspase 3 and caspase 9

H9c2 (7×10^5 cells/well) were seeded in 6-well tissue culture plates and allowed to adhere for 24 h. Thereafter, the medium was replaced with fresh medium and cells were treated as described. Total proteins were extracted from cells by freeze/

thawing in lysis buffer (containing Tris-HCl 50 mM pH 7.4, 50 mM NaF, 150 mM NaCl, 1 % Nonidet P40, 1 mM phenylmethylsulfonylfluoride, 0.2 mM sodium orthovanadate, 1mM EDTA and protease inhibitors). Protein concentrations were determined with the Bio-Rad protein assay (BIO-RAD, Milan Italy), and 50 µg protein/lane was loaded onto an acrylamide gel and separated by SDS-PAGE in denaturing conditions. Blots were incubated, over night, with primary antibody anti-procaspase 3 and anti-caspase 9 (each diluted 1:200; from Santa Cruz Biotechnology, DBA Italy). GAPDH (1:1000) was used as loading control. After incubation with the primary antibodies and washing in TBS/0.1 % Tween, the appropriate secondary antibody, either anti-rabbit (diluted 1:5.000), was added for 1h at room temperature. Immunoreactive protein bands were detected by chemiluminescence using enhanced chemiluminescence reagents (ECL) in LAS 4000 (GE Healthcare). Western blot data were quantified by using ImageJ Software.

1.2.6 Immunofluorescence Analysis with Confocal Microscopy

For immunofluorescence assay, H9c2 cells were seeded on coverslips in 12-well plate (10^4 cells/well) and allow to grow for 24 h; thereafter, the medium was replaced with fresh medium and cells were treated with CoCl_2 (50-100-150 µM) for

3 or 6 h, with or without Radicicol (1 μ M). Then, cells were fixed with 4 % paraformaldehyde in PBS for 15 min and permeabilized with 0.1 % triton X in PBS for 15 min. After blocking with BSA and PBS for 1 h, cells were incubated with rabbit anti- HIF-1 α antibody (TEMA Ricerca-Origene), mouse anti-Cx43 antibody (Santa Cruz Biotechnologies, 1:250) and rabbit anti-TOM20 (1:250) for 2 h at room temperature. The slides were then washed with PBS for three times and fluorescein-conjugated secondary antibody (FITC) or Texas red-conjugated secondary antibody were added for 1 h, DAPI was used for counterstaining of nuclei. Coverslips were finally mounted in mounting medium and fluorescent images were taken under the laser confocal microscope (Leica TCS SP5).

1.2.7 Measurement of Intracellular calcium Signaling

Intracellular calcium concentrations were measured using the fluorescent indicator dye Fura 2-AM, the membrane- permeant acetoxymethyl ester form of Fura 2. Briefly, H9c2 (3 \times 10⁴ cells/well) were seeded in 6-well tissue culture plates and allowed to adhere for 24 h. Thereafter, the medium was replaced with fresh medium and cells were treated as described. After incubation period (3 or 6 h), cells were washed in phosphate buffered saline (PBS), re-suspended in 1 ml of Hank's balanced salt solution (HBSS) containing 5 μ M Fura 2-AM for 45 min.

Thereafter, cells were washed with the same buffer to remove excess Fura 2-AM and incubated in calcium-free HBSS/0.5 mM EGTA buffer for 15 min to allow hydrolysis of Fura 2-AM into its active-dye form, Fura 2. H9c2 cells then were transferred to the spectrofluorimeter (Perkin-Elmer LS-55). Treatment with Ionomycin (1 μ M final concentration), or with carbonyl cyanide p-trifluoromethoxy-pyhenylhydrazone (FCCP, 50 nM final concentration) was carried out by adding the appropriate concentrations of each substance into the cuvette in calcium-free HBSS/0.5 mM EGTA buffer. The excitation wavelength was alternated between 340 and 380 nm, and emission fluorescence was recorded at 515 nm. The ratio of fluorescence intensity of 340/380 nm (F340/F380) is strictly related to intracellular free calcium [Popolo et al., 2011]. Results are indicated as delta increase in fluorescence ratio (F340/F380 nm) induced by ionomycin-basal fluorescence ratio (F340/F380 nm) or FCCP-basal fluorescence ratio (F340/F380 nm).

1.2.8 Measurement of Mitochondrial Superoxide Evaluation with MitoSOX Red

Mitochondrial superoxide formation was evaluated by MitoSOX Red. Briefly, H9c2 (4.0×10^5 cells/well) were plated in 6-well tissue culture plates and allowed to adhere for 24 h. Thereafter, the medium was replaced with fresh medium and cells were treated as described. After incubation period, MitoSOX Red (2.5

μM) was added for 15 min at 37°C before fluorescence evaluation by means of flow cytometry. This indicator is a fluorogenic dye for highly selective detection of superoxide in the mitochondria of live cells and, once targeted to the mitochondria, it is oxidized by superoxide and exhibits red fluorescence. MitoSOX is readily oxidized by superoxide but not by other ROS-generating systems. Cells fluorescence was evaluated using a fluorescence-activated cell sorting and analyzed with Cell Quest software.

1.2.9 Measurement Mitochondrial Membrane Depolarization with TMRE

Mitochondrial permeability transition pore (mPTP) opening was measured with FACS scan by means of the fluorescent dye, tetramethylrhodamine methyl ester (TMRE). Due to its positive charge, TMRE readily accumulates in active mitochondria in inverse proportion to $\Delta\psi_m$ according to the Nernst equation. For these experiments H9c2 (4.0×10^5 cells/well) were seeded in 6-well tissue culture plates and allowed to adhere for 24 h. Thereafter, the medium was replaced with fresh medium and cells were treated as described. Cells were then collected, washed twice with phosphate buffer saline (PBS) and then incubated in PBS containing TMRE (5 nM) at 37°C . After 30 min, cells fluorescence was evaluated using a fluorescence-activated cell sorting and analyzed with Cell Quest software.

1.2.10 Cytochrome c release detection by cytofluorometry

Cytochrome c was checked by fluorescence-activated cell sorting (FACSscan; Becton–Dickinson). H9c2 cells were cultured in a 6-well plate ($4,5 \times 10^5$ cells/well) and allow to grow for 24 h; thereafter, the medium was replaced with fresh medium and cells were treated as described. After incubation period, cells were harvested with scraper and treated with permeabilization buffer (containing 2 % FBS and PBS in the presence of sodium azide 0.1 %, 4 % formaldehyde and Triton X 0.1 %) after the treatment with fixing buffer (containing 2 % FBS and PBS in the presence of sodium azide 0.1 %, 4 % formaldehyde) for 20 min. The permeabilization of cells was performed for 30 min and then anti-cytochrome c antibody was added. Anti-rabbit FITC antibody was used as a secondary antibody (eBioscience, CA, USA). Cells were then washed twice with fixing buffer and then analyzed by means of FACS. Data obtained were analyzed by means of Cell Quest software. Results were shown as percentage of positive cells.

1.2.11 Analysis of apoptosis

Hypodiploid nuclei were analysed using propidium iodide (PI) staining by means of FACs. Briefly, cells were cultured in a 6-well plate ($4,5 \times 10^5$ cells/well) and allow to grow for 24 h; thereafter, the medium was replaced with fresh medium and

cells were treated as described. After incubation period, cells were washed in phosphate buffered saline (PBS) and resuspended in 500 μ L of a solution containing 0.1% sodium citrate, 0.1% Triton X-100 and 50 μ g/mL PI. After incubation at 4°C for 30 min in the dark, cell nuclei were analysed by means of FACS using CellQuest software. Cellular debris were excluded from the analysis by raising the forward scatter threshold, and the DNA content of the nuclei was registered on a logarithmic scale. Data are expressed as the percentage of cells in the hypodiploid region.

1.2.12 Statistical Analysis

Statistical analysis was performed with the aid of commercially available software GraphPad Prism4 (GraphPad Software Inc., San Diego CA, USA). Results are expressed as mean \pm S.E.M. of at least three independent experiments, each performed in duplicate. Statistical analysis was performed by Student's t test. A value of $p < 0.05$ was considered as statistically significant.

1.3 Results

1.3.1 CoCl₂-induced chemical hypoxia

CoCl₂ mimics the hypoxic/ischaemic condition and is a simple and validated *in vitro* tool to study the molecular mechanisms driven by hypoxia [Goldberg et al., 1988]. Cells respond to hypoxia by activation of the hypoxia-inducible factor HIF-1 α , a transcription factor that modulates the expression of genes involved in angiogenesis, survival, metabolism and cell migration [Pennacchietti et al., 2003]. Immunofluorescence analysis confirm the induction of hypoxia in cells treated with CoCl₂ at 50-100-150 μ M for 3 or 6h. In fact, a marked increase of HIF-1 α levels were observed, both in absence and in presence of Radicicol (1 μ M) (Figure 8A). Furthermore, by means of MTT we observed that in our experimental model cells mortality was lower than 50% (Figure 8B).

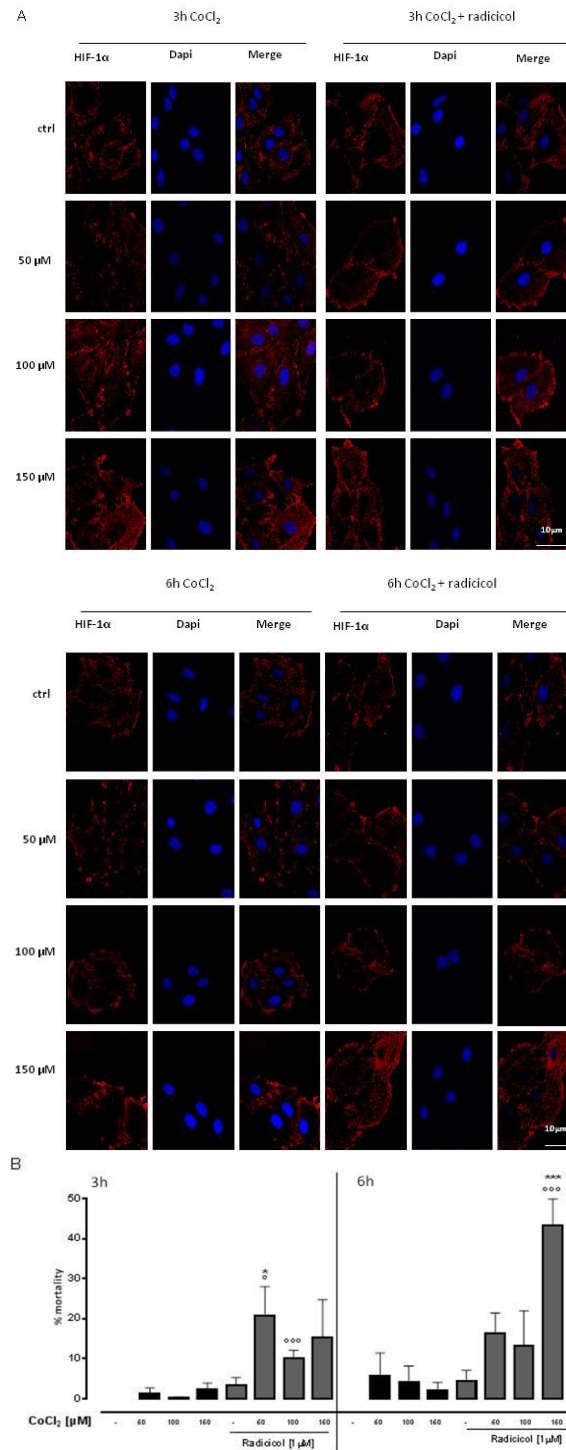


Figure 8: CoCl₂ induces hypoxic state. CoCl₂ (50-100-150 μ M) was administered for 3 and 6 h and H9c2 cells were stained with HIF-1 α (red) and nucleus with DAPI (blue) and were determined by Immunofluorescence analysis. Where indicated, Radicicol (1 μ M) was administered 30 minutes before CoCl₂. Scale bar, 10 μ m. A representative of three experiments was shown. The panel B shows the cytotoxicity measuring the cell mortality after treatment with MTT assay. Cell viability = absorbance of treated sample/absorbance of control. Cells mortality was calculated as: % mortality = 100-[100x(OD treated/OD control)]. Results were analyzed by Student's t test. *p<0.05 and ***p<0.001 vs non-treated; °p<0.05 and °°°p<0.001 vs cells treated with Radicicol alone.

1.3.2 CoCl₂ increased mitochondrial Cx43 expression

Western blot analysis showed a significant ($p < 0.05$) increase of mCx43 expression in CoCl₂-treated H9c2 cells already evident at 3h. Pre-treatment with Radicicol, significantly ($p < 0.05$) reduced CoCl₂-induced mCx43 over-expression at either experimental times (Figure 9A).

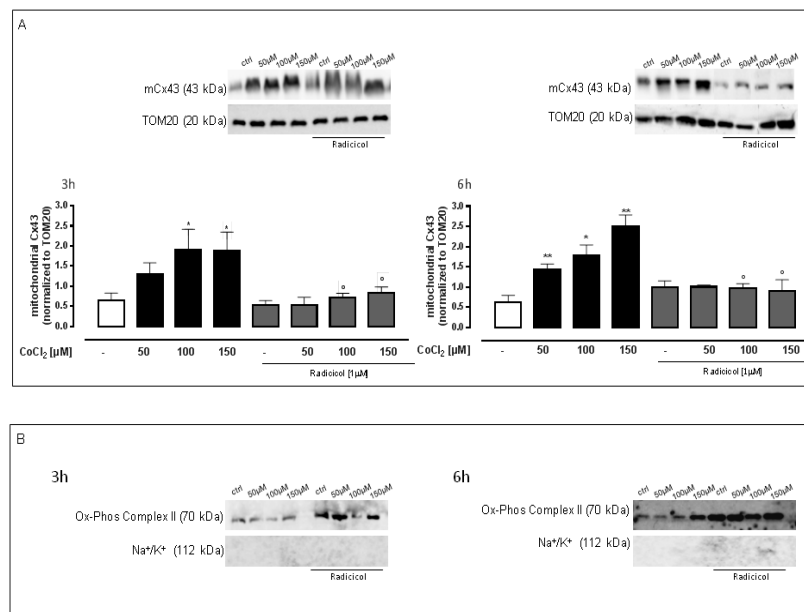


Figure 9: CoCl₂ increases mitochondrial Cx43 expression. CoCl₂ (50-100-150 μM) was administered for 3 and 6 h in H9c2 cells and mCx43 expressions were detected by Western blot analysis. TOM20 protein expression was used as loading control (A). Results are expressed as mean ± S.E.M. from at least three independent experiments each performed in duplicate. Data were analyzed by Student's t test. * $p < 0.05$, ** $p < 0.005$ vs non-treated; ° $p < 0.05$ vs cells treated with Radicicol alone.

Representative Western blots of Na⁺/K⁺ ATPase and Ox-Phos Complex II were used as markers, respectively, to demonstrate the purity of the mitochondrial extracts (B).

Data were confirmed by immunofluorescence analysis which revealed that CoCl₂ administration induced an increase in mCx43 localization while Radicicol reduced this effect (Figure 10).

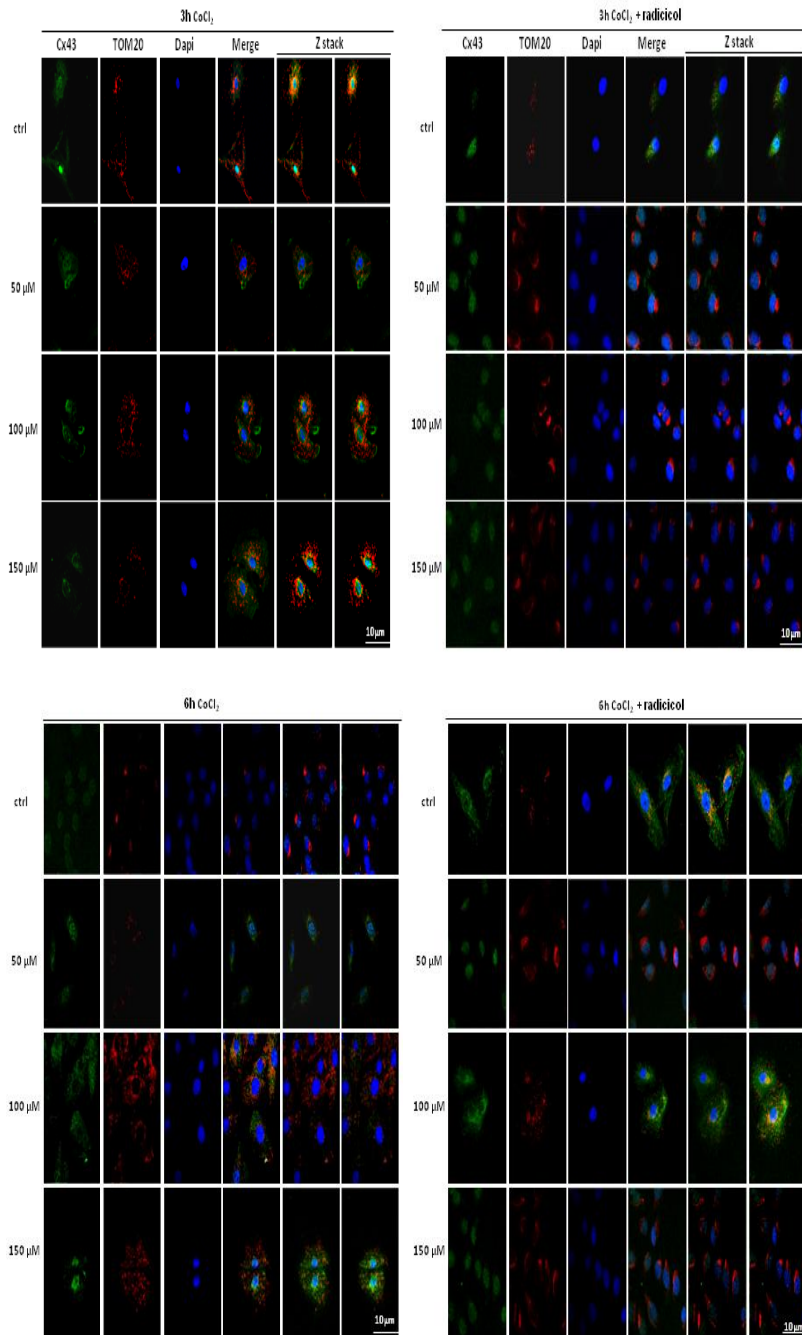


Figure 10: CoCl₂ increases mitochondrial Cx43 localization. CoCl₂ (50-100-150 μM) was administered for 3 and 6 h and H9c2 cells and mitochondrial localization of Cx43 was detected using immunofluorescence assay at confocal microscopy. Where indicated, Radicicol (1 μM) was administered 30 minutes before CoCl₂. The images were obtained through software-generated reconstructions continuously acquiring overlapping (Z stack) images to get the whole cell image. Scale bar, 10 μm. A representative of three experiments was shown.

1.3.3 The inhibition of Cx43 translocation on mitochondria increased Mitochondrial Superoxide Production

The mitochondrial superoxide production was checked by MitoSOX red. Flow cytometry analysis showed that the CoCl₂ (50-100-150μM) treatment significantly (p<0.05) increased mitochondrial superoxide production at both experimental times. Radicicol (1μM) pre-treatment, increases CoCl₂-induced superoxide production. This effect was significant (p<0.05) only at 6h, even if the amount of mitochondrial superoxide production in H9c2 pre-treated with Radicicol at 3h was comparable to those of cells treated for 6h with CoCl₂ alone (Figure 11).

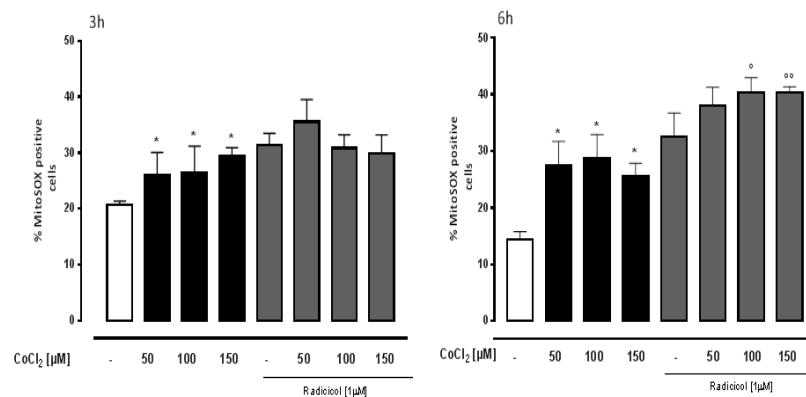


Figure 11: Radicicol increases mitochondrial ROS production in CoCl₂ treated H9c2 cells. Superoxide production by mitochondria was evaluated by means of the probe MitoSOX Red in H9c2 cells by flow cytometry analysis. CoCl₂ (50-100-150μM) was administered for 3 and 6 h. Where indicated, Radicicol (1 μM) was administered 30 minutes before CoCl₂. Mitochondrial superoxide production was expressed as mean ± S.E.M. of percentage of MitoSOX positive cells of at least three independent experiments each performed in duplicate. Data were analyzed by Student's t test. *p<0.05 vs non-treated, °p<0.05 and °°p<0.005 vs cells treated with Radicicol alone.

1.3.4 CoCl₂ induces calcium homeostasis alteration

Intracellular calcium concentrations was evaluated by means of FURA 2-AM in Ca²⁺-free incubation medium (containing 0.5 mM EGTA). CoCl₂-treated cells showed alteration in intracellular Ca²⁺ levels. In fact, delta increase in intracellular Ca²⁺ induced by Ionomycin in CoCl₂-treated cells was significantly (p<0.05) higher than control cells at all experimental time points, indicating higher levels of Ca²⁺ in cellular stores. Pharmacological inhibition of Cx43 translocation on mitochondria by Radicicol significantly affected intracellular Ca²⁺ homeostasis. In fact, in Radicicol pre-treated cells, delta increase in intracellular Ca²⁺ was significantly higher (p<0.05) than cells treated with CoCl₂ alone (Figure 12A). In order to analyze the involvement of mitochondrial Ca²⁺ content, cells were incubated with CoCl₂ alone or pre-treated with Radicicol and then the mitochondrial calcium depletory, carbonyl cyanide p-trifluoromethoxyphenylhydrazone FCCP (50 nM), was added. As reported in Figure 12B, in CoCl₂-treated H9c2 cells delta increase in intracellular Ca²⁺ induced by FCCP was higher than control cells. In Radicicol pre-treated cells, delta increase in intracellular Ca²⁺ was significantly (p<0.05) higher than cells treated with CoCl₂ alone, indicating higher levels of Ca²⁺ in mitochondria of Radicicol pre-treated cells both at 3h and 6h.

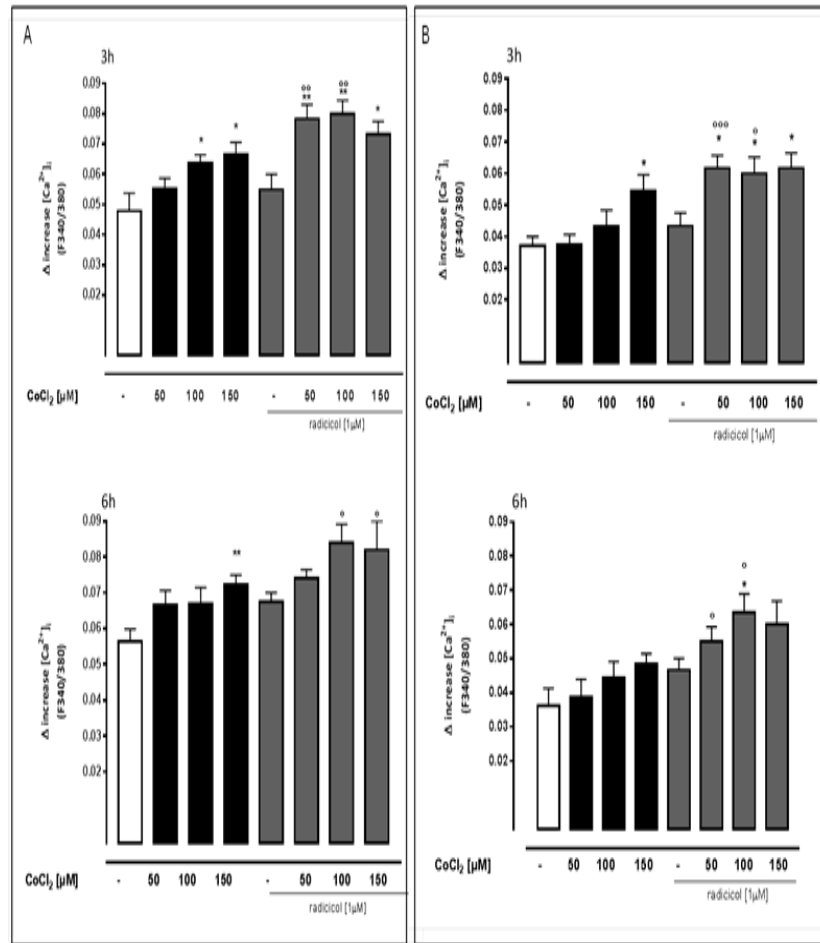


Figure 12: Radicol increases mitochondrial calcium concentrations in CoCl₂ treated H9c2 cells. CoCl₂ (50-100-150 μM) was administered for 3 and 6 h. Where indicated, Radicol (1 μM) was administered 30 minutes before CoCl₂. Intracellular calcium content was evaluated on H9c2 cells in calcium-free medium by means of Ionomycin (1 μM) (panel A). Effect of CoCl₂ on mitochondrial calcium pool was evaluated on H9c2 cells in calcium-free medium in presence of FCCP (50 nM) (panel B). Results are expressed as mean ± S.E.M. of delta (δ) increase of FURA 2 ratio fluorescence (340/380nm) from at least three independent experiments each performed in duplicate. Data were analyzed by Student's t test. *p<0.05 and **p<0.005 vs non-treated; ^{oo}p<0.005 and ^{ooo}p<0.001 vs cells treated with Radicol alone.

1.3.5 The inhibition of Cx43 Translocation Enhanced Mitochondrial Membrane Depolarization

CoCl₂ (50-100-150μM) administration induced the opening of the mitochondrial transition pore, as demonstrated by means of TMRE. In fact, after 3 h of CoCl₂ treatment, we observed an increase of mitochondrial membrane depolarization. But it is interesting to note that inhibition of mCx43 translocation accelerates mitochondrial membrane depolarization. In fact, as reported in Figure 13, in Radicicol pre-treated cells at 3 h mitochondrial membrane depolarization values were higher than those of cells treated for 3h with CoCl₂ alone and comparable to those observed in H9c2 treated with CoCl₂ alone for 6h.

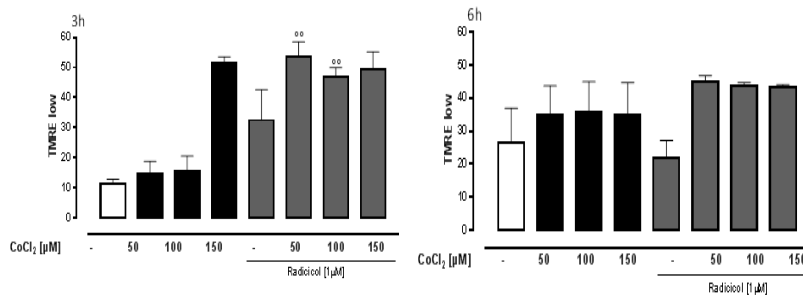


Figure 13: Radicicol increases CoCl₂-induced mitochondrial membrane potential collapse in H9c2 cells. CoCl₂ (50-100-150μM) was administered for 3 and 6 h. Where indicated, Radicicol (1 μM) was administered 30 minutes before CoCl₂. The mitochondrial membrane potential was evaluated by flow cytometry analysis with tetramethylrhodamina ethyl ester (TMRE), a cationic dye that gives a strong fluorescence signal. Results are expressed as mean ± S.E.M. of fluorescence intensity of at least three independent experiments each performed in duplicate. Data were analyzed by Student's t test. **p<0.005 vs cells treated with Radicicol alone.

1.3.6 Inhibition of Cx43 translocation to mitochondria enhances CoCl₂-induced apoptotic response

Jung and co-workers [2004] report that one of the causes of cell death could be mitochondrial membrane permeabilization, therefore we analysed the apoptotic response in our experimental conditions. Treatment with CoCl₂ leads to an increase of the cytochrome c release (Figure 14A) and in the number of aplodyploid nuclei (Figure 14B), as compared with untreated cells. In agreement with the activation of the mitochondrial apoptosis canonical way, Western blot analysis showed a significant and dose-dependent reduction of procaspase 3 levels and an increase caspase 9 levels in CoCl₂-treated cells (Figure 14C). Radicicol pretreatment significantly ($p < 0.05$) reduced cytochrome c release and the number of hypodyploid nuclei induced by CoCl₂ at both experimental times.

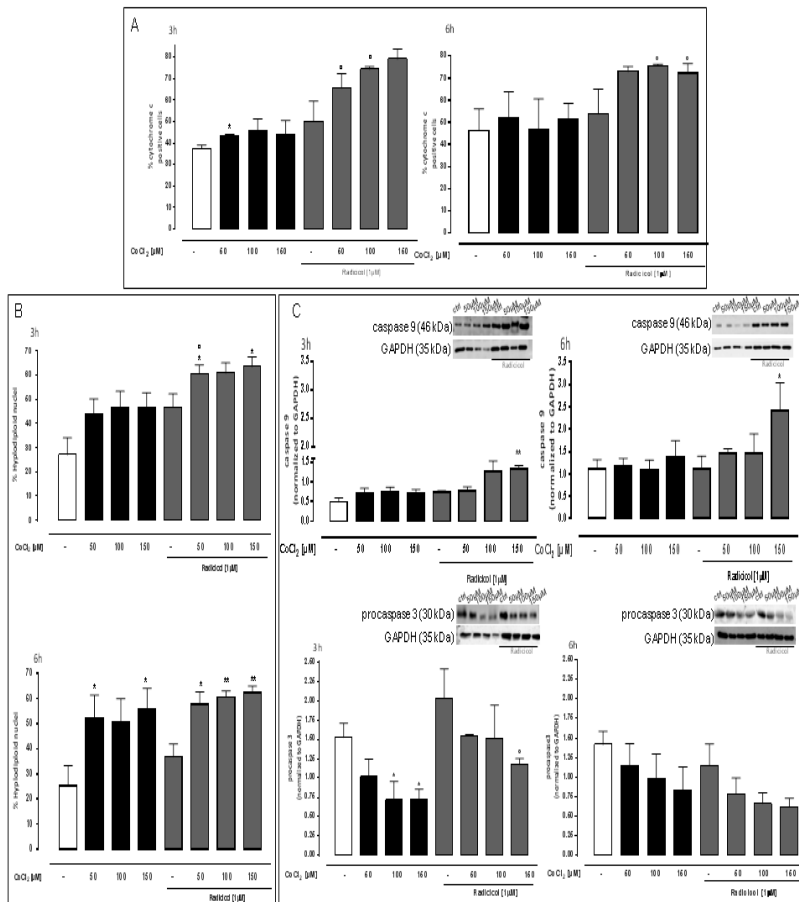


Figure 14: Radicol increased the trigger of the apoptotic pathway induced by CoCl₂ in H9c2 cells. CoCl₂ (50-100-150μM) was administered for 3 and 6 h, where indicated, Radicol (1 μM) was administered 30 minutes before CoCl₂. Cytochrome c level into the cytosol was checked by flow cytometry analysis. Results are expressed as mean ± S.E.M. of percentage of cytochrome c positive cells from at least three independent experiments each performed in duplicate (panel A). H9c2 were stained by propidium iodide and fluorescence of individual nuclei was measured by flow cytometry. Results are expressed as mean ± S.E.M. of percentage of hypodiploid nuclei from at least three independent experiments each performed in duplicate (panel B). Caspase 9 and procaspase 3 expressions were detected by Western blot analysis; GAPDH protein expression was used as loading control. Results are expressed as mean ± S.E.M from at least three independent experiments each performed in duplicate (panel C). Data were analyzed by Student's t test. *p<0.05 and **p<0.005 vs non-treated; °p<0.05 vs cells treated with Radicol alone.

1.4 Discussion

GJ plaques are typically observed in the heart at the intercalated disks of adjacent cardiomyocytes [Revel & Karnovsky, 1967; Severs, 1990] where they facilitate electrical current flow that coordinates cardiomyocyte contraction to sustain its pump function [Severs et al., 2004]. In particular, Cx43 forms hemichannels, which are predominantly closed in healthy myocardium [Goodenough et al, 2004; Kryska et al., 2005]. However, they can open in response to electrical and chemical triggers, most notably during ischemia and inflammatory conditions [Saez et al., 2005; Saez & Leybaert, 2014; Wang et al., 2012a; Wang et al., 2013a; Wang et al., 2013b]. A prolonged opening of Cx43 hemichannels during ischemia may lead to loss of ionic gradients, excessive Ca^{2+} entry, cell swelling and cellular damage. Apart from being present at the sarcolemma, Cx43 has been identified in mitochondria of cardiomyocytes, where it plays a pivotal role in mediating the cardioprotective effect of ischemic preconditioning [Boengler et al., 2005].

Rodriguez-Sinovas and co-workers [2006] demonstrated that ischemic preconditioning induces Cx43 translocation from cytosol to mitochondria with a mechanism that involves Hsp90 and TOM20. MCx43 is important in maintaining cellular mitochondrial homeostasis via regulating energy balance and calcium homeostasis [Wu et al., 2009], eliminating ROS [Jezek

et al., 2014], and regulating cellular apoptosis [Dando et al., 2013], thereby providing cellular protective effects.

Here, we evaluated the influence of mCx43 in *in vitro* hypoxia model. Hypoxia was induced by means of Cobalt Chloride (CoCl₂), a well-known hypoxia mimetic agent [Shi-Yun et al., 2017], that is able to mimic the hypoxic response in many cellular process such as oxidative stress, dissipation of mitochondrial membrane potential, dysregulation of calcium homeostasis and consequent triggering of apoptosis [Wang et al., 2013]. In our experimental model, CoCl₂ is able to induce hypoxia, like demonstrated by HIF-1 α increased expression, without affecting cell viability in a drastic manner. In fact, we chose to use CoCl₂ doses and incubation times that could induce hypoxia but did not give an excessive mortality because our goal was to observe early responses to induced damage.

As demonstrated by Western blot analysis, and then confirmed by Immunofluorescence, in our experimental conditions CoCl₂ induces an increase of mCx43 expression to mitochondria with a mechanism that involves the well designed Hsp90/TOM20 machinery system. In fact, blocking Cx43 interaction with Hsp90, through Radicol, significantly reduced the mitochondrial import of Cx43. It is well known that the CoCl₂-induced hypoxia is characterized by dysregulation of calcium homeostasis, increase of reactive oxygen species, cell necrosis

and induction of pro-apoptotic signaling pathways [Wang et al., 2013]. MCx43 impacts on respiratory function [Boengler et al., 2012] and modulates the calcium overload, mitochondrial permeability transition and cell death [Srisakuldee et al., 2014]. Our data demonstrate that CoCl_2 induces an increase in intracellular Ca^{2+} levels in H9c2 cells, as revealed by means of FURA 2-AM, instead inhibition of Cx43 translocation to mitochondria significantly rises the intracellular levels of $[\text{Ca}^{2+}]$, resulting in an increase of mitochondrial Ca^{2+} accumulation induced by CoCl_2 . The role of mCx43 in calcium homeostasis in hypoxic conditions is controversial. Gadicherla and co-workers indicate that mCx43 directly contribute to mitochondrial calcium entry/overload thus triggering cell injury/death pathways [2017]. On the other hand, other authors indicate that mCx43 exerts its cardioprotective effects by mitigating calcium overload, mitochondrial permeability transition and cell death [Srisakuldee et al., 2014]. This cardioprotective effect seems to be related to the increased mitochondrial calcium uptake and storage capacity during ischemia that helps to delay a rise in cytosolic calcium levels [Garcia-Dorado et al., 2012]. Our data support this hypothesis. Indeed, Jung and co-workers [2001] demonstrated that calcium levels are closely associated in mitochondrial ROS production and this suggests that chronic hypoxia-induced cell damages are related to mitochondrial

dysfunction. Here, we observed that CoCl_2 induces an increase in mitochondrial oxygen radical species, as demonstrated by means of MitoSOX. The inhibition of Cx43 translocation to mitochondria by Radicicol, significantly increases the effect of CoCl_2 . It is well known that both mitochondrial calcium overload and ROS production induce mitochondrial membrane depolarization [Gadicherla et., 2017]. In fact, data obtained by means of TMRE showed that in our experimental conditions CoCl_2 -induced mitochondrial membrane depolarization was more evident and faster in presence of the pharmacological inhibitor of Cx43 translocation on mitochondria. Hypoxia of cardiomyocytes cause cardiac dysfunction due to its triggering cell injury and apoptosis. In fact, as demonstrated by our data, CoCl_2 administration induces cytochrome c release, causing a significant increase of apoptotic process, as shown by FACS analysis with the use of propidium iodide. Furthermore, CoCl_2 induces an increase of caspase 9 levels and a concomitant reduction of procaspase 3 levels. Use of Radicicol significantly increases CoCl_2 -induced apoptotic signaling.

In conclusion, our data obtained suggest that mCx43 is essential for the cytoprotection stultify the apoptotic process induced by chemical hypoxia and suggest that the presence of mCx43 is of utmost importance for cardioprotective pathways being functional.

Chapter II

Involvement of Connexin 43 in Calcium

Impairment induced by Doxorubicin in a short-term mouse model

2.1 Introduction

Anthracyclines, used alone or in combination with other chemotherapeutic agents, are a class of antitumour drugs widely used for the treatment of a variety of cancers, such as breast cancer, lymphoma and melanoma [Hrdina et al., 2000]. Anthracycline agents are antibiotics isolated from soil microbe *Streptomyces peucetius* [Jain et al., 2017] and the commonly used include Doxorubicin (DOXO), Daunorubicin, and Epirubicin [Gewirtz et al., 1999]. DOXO is one of the most widely used and successful prescribed broad-spectrum chemotherapeutic [Smuder et al., 2013], but, unfortunately, its usage is limited by the cumulative, dose-dependent cardiomyopathy. In fact, one major side effect of this class of chemotherapeutic drugs is cardiotoxicity [Octavia et al., 2012], leading to dilated cardiomyopathy and heart failure [Wong et al., 2013]. The mechanisms of DOXO-induced cardiotoxicity are complicated and it is associated with the production of ROS and oxidation of lipids, DNA and proteins [Nordgren et al., 2014],

mitochondrial dysfunction, myofibril degeneration [Kavazis et al., 2016; Ghigo et al., 2016] and altered calcium handling by sarcoplasmic reticulum [Zhang et al., 2012]. Generation of ROS has been reported as the main mechanism that explains the pathophysiology of DOXO-induced cardiomyopathy [Fouad et al., 2011]. Similarly, other mediators such as Angiotensin II have also been found to play a critical role in the development of DOXO-induced cardiomyopathy [Toko et al., 2002]. The mechanisms of DOXO has been found to involve the activation of DOXO molecule into a more reactive semiquinone by mitochondrial complex I, resulting in increased oxidative stress [Carvalho et al., 2014]. However, Ren and co-workers [2012] reported that DOXO induces activation of both extrinsic and intrinsic apoptotic signaling pathways. Cardiac toxicity of DOXO was recently reported on electrocardiogram with a significant increase in heart rate, elevation of the ST segment, prolongation of the QT interval and an increase in T wave amplitude [Ammar et al., 2013]. Indeed, its disturbances in cardiac rhythm [Ferrans et al., 1997], changes in blood pressure [Medrano et al., 2001], reduction of ejection fraction and contractile function [Chatterjee et al., 2010] and cardiac dilation [Takemura et al., 2007], are often not clinically evident until the late stages.

Anthracycline cardiotoxicity is classified as acute and chronic. Acute cardiotoxicity occurs during or soon after initiation of therapy. This is usually transient and self-limiting with a myopericarditis like picture, non-specific repolarization changes on ECG, dysrhythmias, troponin elevation, and transient LV dysfunction [Dazzi et al., 2001]. Chronic cardiotoxicity is arbitrarily classified as type 1 or early onset (typically detected within one year of completion of chemotherapy) and type 2 or late-onset (usually detected after the first year with an unlimited time frame of up to decades after completion of chemotherapy) [Lipshultz et al., 1991; Lipshultz et al., 2005]. Majority of the patients develop chronic cardiotoxicity within the first year of completing therapy [Cardinale et al., 2015]. The total lifetime cumulative dose of anthracycline is the most important determinant of anthracycline cardiotoxicity [Von Hoff et al., 1979]. DOXO-induced cardiotoxicity is mainly related to accumulation of the repetitive doses required by the treatments, in fact total DOXO concentration cannot exceed 500 mg/m². Recent evidence indicates that the damage caused by anthracyclines on cardiomyocytes is an early event, already evident after a single administration [Menna et al., 2008]. But until now most of the studies published report only the effects of long-term DOXO-administration [Zhang et al., 2014; O'Connell et al., 2017].

DOXO-induced cardiomyopathy is characterized by abnormal calcium homeostasis. Recently it has been demonstrated that DOXO administration is able to induce calcium dysregulation and Cx43 re-arrangement in a rat cardiomyoblast cell line already evident after a short-term administration [Pecoraro et al., 2015 b]. Cx43 is functionally associated with calcium and Cx43 remodelling might be responsible for intracellular calcium overloading induced by DOXO, thus resulting in ischemic arrhythmia [Kristia'n et al., 1998]. On the basis of these data, we analyzed the effect of DOXO-administration on Cx43 expression and localization in a short-time mouse model of DOXO-induced cardiotoxicity.

2.2 Materials and Methods

2.2.1 Materials

DOXO was purchased from Baxter manufacturing S.p.a. (Officina di Sesto Fiorentino, Florence, Italy). Where not indicated otherwise, antibodies used were purchased from Santa Cruz Biotechnology (DBA, Milan, Italy), and all other products were purchased from Sigma (Milan, Italy).

2.2.2 Animals

Six week old female C57BL/6j (weighting 20–22 g) were purchased from Charles River (Lecco, Italy). All experimental procedures that involve animals have been conducted in agreement with the Italian and European Community Council for Animal Care (DL. no. 26/2014 protocol number of Ministerial approval DGSAF 13788-A 02/07/2015) and in accordance with the guidelines of the Guide for the Care and Use of Laboratory Animals of the National Institutes of Health.

2.2.3 Experimental Protocols

C57BL/6j mice were randomly divided in three groups (n = 6 for each experimental group). The doses used were 2 and 10 mg/kg [Xujie et al., 2012; Wided et al., 2014] and they corresponded to 6.142 and 30.8 mg/m² respectively [Freireich et al., 1997].

First Group: received one DOXO administration (2 or 10 mg/kg i.p.) and were sacrificed 24 h after the treatment;

Second Group: received two DOXO administrations (2 or 10 mg/kg i.p.) once a day for two days and were sacrificed three days after the first administration;

Third Group: received three DOXO administrations (2 or 10 mg/kg i.p.) once a day for three days and were sacrificed seven days after the first administration.

Mice that received saline were used as control group. Cardiac function was monitored echocardiographically at baseline and before sacrifice. At the end of each experimental time, heart samples were collected and prepared for molecular biological analyses.

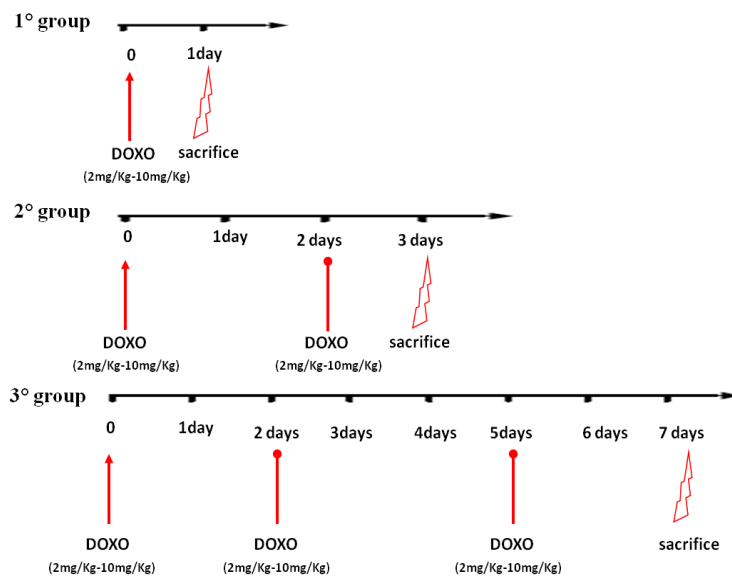


Figure 15: Timetable. C57BL/6j female mice were randomly divided into three groups. The 1st group received a single administration of DOXO (2 mg/Kg and 10 mg/Kg; i.p.) and was sacrificed after 24h; the 2nd group received two administrations of DOXO (2 mg/Kg and 10 mg/Kg; i.p.) once every other day and was sacrificed 3 days after the first injection; the 3rd group received three administrations of DOXO (2 mg/Kg and 10 mg/Kg; i.p.) once every other day and was sacrificed 7 days after the first injection. Control group received saline solution. At the end of experimental time, mice were sacrificed and the heart was removed and frozen for biochemical analysis.

2.2.4 Echocardiogram

Mice were lightly anesthetized with 1–1.5% of isoflurane in oxygen until the heart rate stabilized to 400–500 beats per minute. Echocardiography was performed using VEVO (VisualSonic, Toronto, (Canada) instrument. Ejection fraction (EF), Fractional shortening (FS), Left Ventricular End-Diastolic-Diameter (LVEDD), and Left Ventricular End-Systolic Diameter (LVESD) were calculated using the VEVO analysis software (Toronto, Canada).

2.2.5 Histological staining

For histological analyses, hearts were embedded in OCT medium (Bio-Optica, Milan, Italy). Sections (7 μ m) were fixed with acetone and stained either hematoxylin and eosin (H&E staining) to evaluate the cardiac structure following the administration of DOXO. Coverslips were finally mounted in mounting medium and all the photomicrographs were taken at 20 \times magnification under the FluorescenceMicroscope (Axio Vision software).

2.2.6 Protein Extraction and Western Blot Analysis

Total proteins were extracted by homogenization of hearts with a dounce potter in lysis buffer (TRIS-HCl 50 mM, NaCl 500 mM, protease inhibitors, PMSF 0.25 μ M, NaF 50 mM, Na₃VO₄

0.2 mM). Protein concentrations were determined with the Bio-Rad protein assay (BIO-RAD, Milan, Italy). Equal amounts of protein (50 µg) were loaded into an acrylamide gel and separated by SDS-PAGE under denaturing conditions. Blots were incubated with primary antibody anti-Cx43 (Sigma, 1:8000), anti-pCx43 phosphorylate on Ser368 (Santa Cruz, 1:250), anti-sarco/endoplasmic reticulum Ca^{2+} -ATP_{ase} (SERCAII; Santa Cruz, 1:250), anti-phospholamban (PLB; Santa Cruz, 1:200), or anti-glyceraldehyde 3-phosphate dehydrogenase (GAPDH; Santa Cruz, 1:1000, used as loading control) overnight at 4 °C. After incubation period with the primary antibodies, blots were washed in PBS 0.1% Tween. The appropriate secondary antibody anti-rabbit, anti-mouse, or anti-goat (each diluted 1:4000) was added and allowed in incubation for 1 h at room temperature. Immunoreactive protein bands were detected by chemiluminescence using enhanced chemiluminescence reagents (ECL) in LAS 4000 (GE Healthcare, Björkgatan, Sweden).

2.2.7 Mitochondrial Protein Extraction and Western Blot Analysis for Mitochondrial Cx43 and pCx43

Mitochondrial proteins were extracted from homogenized hearts with a dounce potter in lysis buffer (sucrose 250 mM, K⁺ HEPES pH 7.5 20 mM, KCl 10 mM, MgCl₂ 1.5 mM, EDTA 0.1 mM, EGTA 1 mM, protease inhibitors, NaF 50 mM, Na₃VO₄ 0.2

mM, PMSF 100 μ M, DTT 1 mM, digitonin 0.025%) as previously reported [Pecoraro et al., 2015 b; Sardão et al., 2009]. The protein yield was quantified with the Bio-Rad protein assay (BIO-RAD, Milan, Italy). Western blot analysis for Cx43 or pCx43 was performed as described above. Primary antibody anti-TOM20 (Santa Cruz) was used as loading control. In order to verify the purity of mitochondrial protein extraction, a Western blot analysis was performed to evaluate the presence of proteins expressed only in the mitochondria (ox-Phos Complex II, Abcam, 1:7000) and the absence of proteins expressed in other cellular compartments (Na^+/K^+ ATP_{ase}, Abcam, 1:3000) [Boengler et al., 2005].

2.2.8 Primary Cardiomyocytes Isolation and Measurement of Intracellular Ca^{2+} Signaling

Intracellular Ca^{2+} concentrations were measured in primary cardiomyocytes, isolated from hearts of DOXO-treated mice and control mice. Hearts were washed with HBSS 0.1 mM Ca^{2+} (140 mM NaCl, 5.4 mM KCl, 0.44 mM KH_2PO_4 , 0.42 mM Na_2HPO_4 , 4.17 mM NaHCO_3 , 26 mM CaNa-EDTA, 0.10 mM $\text{CaCl}_2 \cdot \text{H}_2\text{O}$, 5.0 mM HEPES and 5.5 mM dextrose). Next, hearts were cut in 1–2 mm sections and incubated at 37 °C in HBSS 0.1 mM Ca^{2+} containing albumin 10 mg/mL, trypsin inhibitor 1 mg/mL, taurine 5 mM, dithiothreitol 0.4 mg/mL, collagenase II 0.6 mg/mL, and papain 0.6 mg/mL for 75 min. After the

incubation period, tissue fragments were removed by filtering the suspension with a 0.70 μ filter. Filtrate was centrifuged to collect the cardiomyocytes. Primary cardiomyocytes were loaded with the ratiometric fluorescent indicator dye FURA2-AM (5 μ M, 45 min, 37 °C) at a cell density of 3×10^4 cells/mL in HBSS 0.1 mM Ca^{2+} . FURA2-AM excess was removed by washing the cells with HBSS and cardiomyocytes were then transferred to a spectrofluorimeter (Perkin-Elmer LS-50). As reported for FURA2-AM, the excitation wavelength was alternated between 340 and 380 nm, and the emission wavelength was 515 nm. The basal F340/F380 ratio was recorded and then treatment with ionomycin (1 μ M), a calcium ionophore; thapsigargin (1 μ M), an inhibitor of sarco(endo)plasmic reticulum; or carbonyl cyanide p-trifluoromethoxyphenylhydrazone (FCCP; 50 nM), a mitochondrial calcium depletory, was added into the cuvette in Ca^{2+} -free HBSS and F340/F380 ratio was recorded 5 min after each stimulus induced. The ratio of fluorescence intensity of 340/380 nm (F340/F380) is strictly related to intracellular free $[\text{Ca}^{2+}]$ [Popolo et al., 2011]. Results are expressed as delta increase of F340/F380, calculated as F340/F380 stimulus - F340/F380 basal.

2.2.9 Immunohistochemical Analysis

For immunohistochemical analyses, frozen cardiac tissues were embedded in OCT compound (Bio-Optica, Milan, Italy). Sections (7 μ m) were incubated with mouse anti-Cx43 (1:250) and rabbit anti-TOM20 (1:250) for 2 h at room temperature. Then the slides were washed three times with PBS and incubated with secondary antibodies (FITC-conjugated anti mouse IgG and Texas red-conjugated anti rabbit IgG) for 1 h. DAPI was used to mark the nuclei. After mounting, coverslips were examined by using a Laser Confocal Microscope (Leica TCS SP5, Wetzlar, Germany).

2.2.10 Statistical Analysis

Data are reported as the mean \pm standard error mean (S.E.M.) of at least three independent experiments. Statistical differences were assessed with Student's t-test. p-values of less than 0.05 was considered significant.

2.3 Results

2.3.1 Cardiac Functions

Mice were subjected to echocardiography at baseline and before the sacrifice to analyze the main parameters of cardiac function. As reported in Table 1, DOXO administration affects Ejection Fraction (EF), Fractional Shortening (FS), Left Ventricular End-Diastolic Diameter (LVEDD) and Left Ventricular End-Systolic Diameter (LVESD) in mice after a single injection of DOXO. Indeed, compared with control mice, DOXO-treated mice exhibited decreased cardiac systolic function as indicated by EF and FS, increased LVEDP and LVESD.

1 st group		Control	2mg/Kg	10mg/Kg
	LVEDD	3,97 ± 0,11	3,92 ± 0,11	4,09 ± 0,10
	LVESD	2,62 ± 0,17	2,77 ± 0,09	3,00 ± 0,06 *
	%EF	62,17 ± 4,1	58,39 ± 1,12 *	52,7 ± 1,38 **
	% FS	30,41 ± 0,72	33,26 ± 2,93	26,76 ± 0,92 *
2 nd group		Control	2mg/Kg	10mg/Kg
	LVEDD	3,94 ± 0,05	3,87 ± 0,05	3,99 ± 0,06
	LVESD	2,78 ± 0,054	2,78 ± 0,05	2,90 ± 0,06 *
	%EF	57,2 ± 1,25	54,63 ± 1,6 *	53,73 ± 1,61 *
	% FS	30,41 ± 0,85	27,95 ± 1,06 *	27,43 ± 1,02 *
3 rd group		Control	2mg/Kg	10mg/Kg
	LVEDD	3,86 ± 0,04	3,94 ± 0,07	3,96 ± 0,06 *
	LVESD	2,73 ± 0,15	2,85 ± 0,06	2,9 ± 0,14 *
	%EF	59,00 ± 4,17	54,4 ± 2,6 *	50,49 ± 4,79 **
	% FS	31,76 ± 1,68	30,97 ± 2,91	25,39 ± 3,02*

Table 1: Effect of DOXO (2 or 10 mg/kg; i.p.) on Left Ventricular End-Diastolic Diameter (LVEDD), Left Ventricular End-Systolic Diameter (LVESD), Ejection Fraction (% EF), and Fractional Shortening (% FS) after a single administration (1th group), two administrations (2nd group), or three administrations (3rd group). Results were expressed as mean ± S.E.M. from 6 mice/group

2.3.2 Histopathological examination

To characterize the cardiotoxicity induced by DOXO, histopathological examination of heart tissue was performed as shown in Figure 16. Hearts from control mice showed regular cell distribution and normal myocardium architecture. Hearts sections of DOXO-treated mice fixed and examined microscopically exhibit vacuolar and granular degeneration, already evident in mice that received a single administration of DOXO.

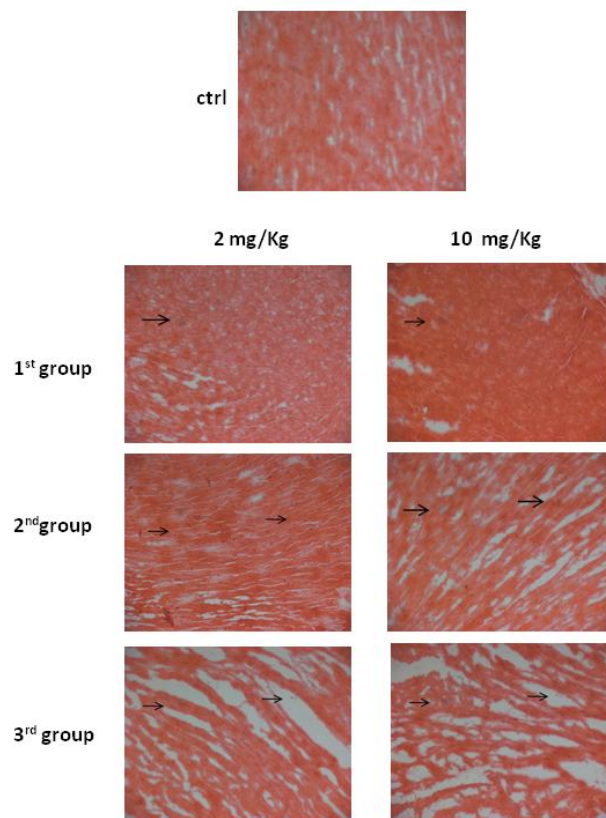


Figure 16: Immunostaining heart section of C57bl/6j mice which received a single administration (1st group), two administrations (2nd group) or three administrations (3rd group) of DOXO (2 mg/kg and 10 mg/kg; i.p.). Hematoxylin (red) and eosin (blue) staining of cardiac sections. All the photomicrographs were taken at 20× magnification. The administration of DOXO destroyed the cardiac structure

2.3.3 Doxorubicin Administration Alters Calcium Homeostasis

It is well known that impairment in $[Ca^{2+}]_i$ plays a pivotal role both in cardiotoxic activity of DOXO [Wallace et al., 2003] and in Cx43 activity [Bol et al., 2017]. In order to evaluate the effects of DOXO treatment on intracellular Ca^{2+} levels in our experimental model, primary cardiomyocytes from hearts of DOXO-treated mice and from control mice were isolated and loaded with the fluorescent dye FURA2-AM in Ca^{2+} -free incubation medium (containing 0.5 mM EGTA). Our data indicate that DOXO treatment increased basal level of $[Ca^{2+}]_i$. Indeed the delta increase in $[Ca^{2+}]_i$ induced by ionomycin, a Ca^{2+} ionophore, in cardiomyocytes from DOXO-treated mice was significantly ($p < 0.05$) lower than that found in cells from control mice at all experimental time points (Figure 17A). An increase in basal Ca^{2+} levels may indicate that the cells are not capable of storing Ca^{2+} in intracellular stores. Accordingly (Figure 17B), delta increase in $[Ca^{2+}]_i$ induced by thapsigargin, an endoplasmic reticulum Ca^{2+} stores depletor, in cardiomyocytes from DOXO-treated mice was significantly lower ($p < 0.001$) than that registered in cardiomyocytes from control mice, even in presence of a single DOXO administration, which may indicate a reduced Ca^{2+} storage in the endoplasmic reticulum. In the same way, the delta increase in

$[Ca^{2+}]_i$ induced by FCCP, a mitochondrial Ca^{2+} depletory, in cardiomyocytes from DOXO-treated mice was significantly ($p < 0.001$) lower than that found in cells from control mice in all experimental groups (Figure 17C), suggestive of less build-up of Ca^{2+} also in the mitochondria. Among all regulatory mechanisms involved in intracellular Ca^{2+} homeostasis, SERCAII plays a pivotal role. Many studies report how changes in the expression and/or activity of SERCAII, regulated by phospholamban (PLB), are altered in many forms of cardiomyopathy [Periasamy et al., 2008]. Therefore, we analyzed the expression levels of SERCAII and PLB in the heart of DOXO-treated mice. Data obtained by Western blot analysis showed a significant ($p < 0.05$) reduction of SERCAII expression always in mice that received a single DOXO administration (Figure 17D) and a concomitant increase in PLB expression (Figure 17E).

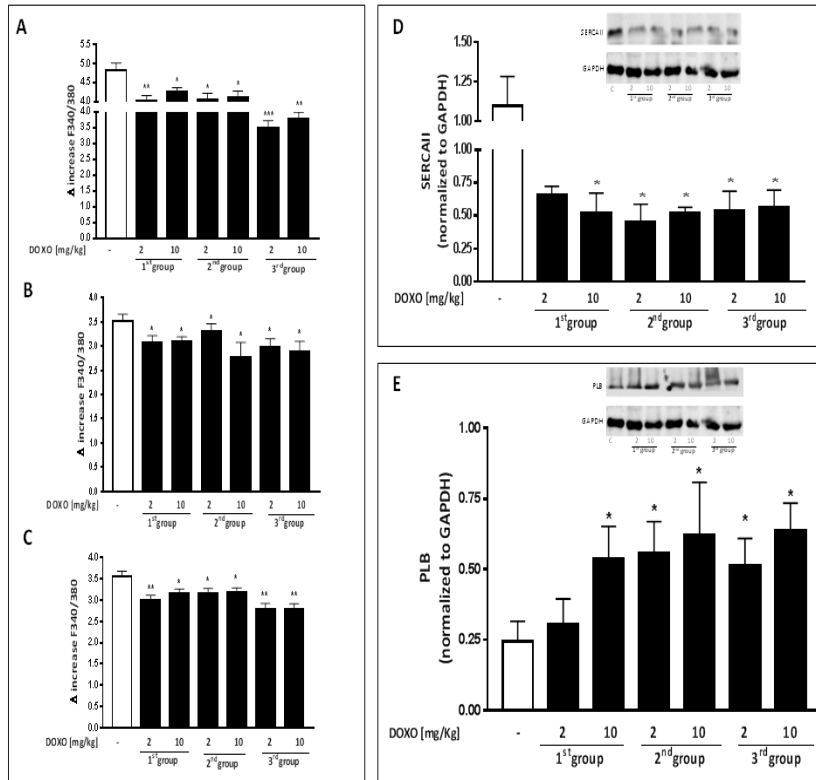


Figure 17. Effect of DOXO on calcium homeostasis. Mice received a single administration (1th group), two administrations (2nd group) or three administrations (3rd group) of DOXO (2 or 10 mg/kg; i.p.) and primary cardiomyocytes were isolated by enzymatic digestion. Intracellular calcium content in cells suspension was evaluated by using ionomycin (1 μ M) (A); reticulum calcium content was evaluated by means of thapsyargin (100 nM) (B) and mitochondrial calcium content was evaluated by using FCCP (50 nM) (C). Results were expressed as mean \pm S.E.M. of delta (δ) increase of FURA-2 AM ratio fluorescence (340/380 nm) from at least three independent experiments each performed in duplicate. Data were analyzed by Student's t-test. * $p < 0.05$, ** $p < 0.005$ and *** $p < 0.001$ vs. control. Effect of DOXO on SERCA II (D) and PLB (E) expression. Mice received a single administration (1th group), two administrations (2nd group), or three administrations (3rd group) of DOXO (2 mg/kg or 10 mg/kg; i.p.) and SERCA II and PLB expressions were detected by Western blot analysis into tissue homogenates from mice; GAPDH protein expression was used as loading control. Values were expressed as mean \pm S.E.M. from at least three independent experiments each performed in duplicate. Data were analyzed by Student's t-test. * $p < 0.05$ vs. control.

2.3.4 Doxorubicin Administration Affects Cx43 Expression and Localization

Besides alterations in Ca^{2+} homeostasis, several forms of cardiomyopathy, such as hypertrophy, and dilated and ischemic cardiomyopathy are also characterized by abnormal Cx43 expression and distribution in the heart [Fontes et al., 2012]. As depicted in Figure 18A, DOXO-treatment induces a decrease of total Cx43 also evident in mice that received a single dose of DOXO. Western blot analysis performed on heart lysates of treated-mice confirmed that, compared to control mice, DOXO-treated mice had a significant ($p < 0.05$) reduction of Cx43 expression, that could be observed in all experimental groups (Figure 18A). Phosphorylation of Cx43 affects its main biological properties [Jeyaraman et al., 2012]. In particular, phosphorylation on Ser368 is linked to metabolic and/or electrical uncoupling of gap junctions [Solan et al., 2009] and induces channels closure [Boengler et al., 2006]. Accordingly, Western blot analysis showed that DOXO-administration significantly ($p < 0.05$) increases the expression of Cx43 phosphorylated on Ser368 (Figure 18B). In addition to the function performed at GJ levels, it has recently been shown that Cx43 is also expressed at mitochondrial level, where it is involved in cardioprotection [Sakurai et al., 2013; Kalvelyte et al., 2003]. MCx43 levels increase in stress conditions such as ischemia-reperfusion [Rodriguez-Sinovas et al., 2006] or

DOXO-induced cardiotoxicity [Pecoraro et al., 2015 b]. Western blot analysis performed on mitochondrial lysates from hearts of DOXO-treated mice confirmed that Cx43 expression on mitochondria significantly ($p < 0.05$) increases in DOXO-treated mice (Figure 18C). Mitochondrial expression of Cx43 phosphorylated on Ser368 significantly ($p < 0.005$) increased in a time dependent-manner in the heart of DOXO-treated mice (Figure 18D).

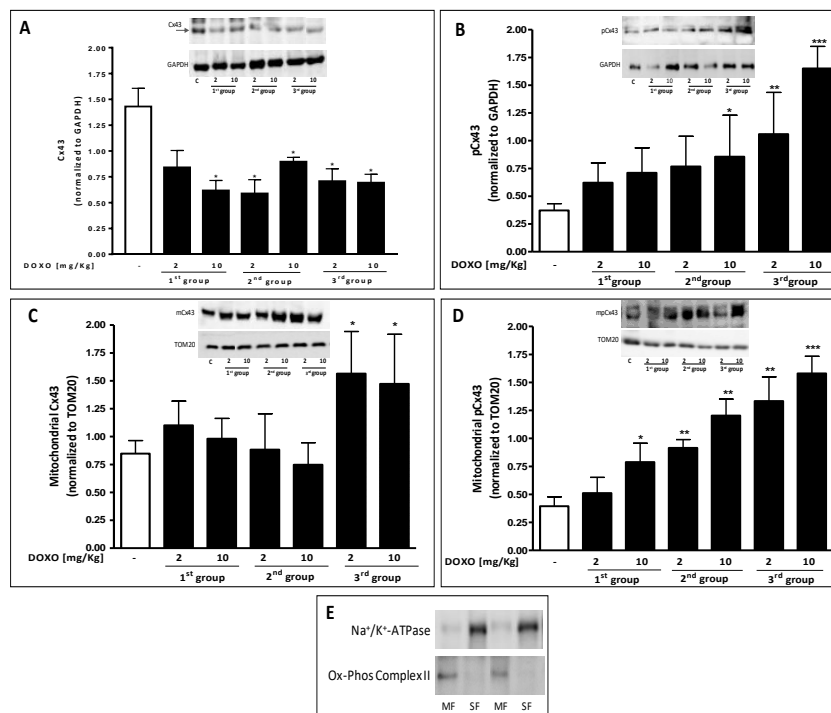


Figure 18. Mice received a single administration (1th group), two administrations (2nd group), or three administrations (3rd group) of DOXO (2 mg/kg and 10 mg/kg; i.p.) and Cx43 and pCx43 expressions were detected by Western blot analysis into tissue homogenates from mice; GAPDH protein expression was used as loading control (A,B); Effects of DOXO on mCx43 (C) and mCx43 phosphorylated on Ser368 (mpCx43) (D) expression were detected by Western blot analysis on mitochondrial protein lysate from mice; TOM20 protein expression was used as loading control. Values were expressed as mean \pm S.E.M. from at least three independent experiments each performed in duplicate. Values are expressed as mean \pm S.E.M. from at least three independent experiments each performed in duplicate. Data were analyzed by Student's *t*-test. * $p < 0.05$, ** $p < 0.005$ and *** $p < 0.001$ versus control. Representative Western blots of Na⁺/K⁺ATPase and Ox-Phos Complex II were used as markers of sarcolemma (SF) and mitochondria (MF), respectively, to demonstrate the purity of the mitochondrial extracts (E).

Immunofluorescence analysis performed on heart sections double-stained for Cx43 and TOM20, as a marker of mitochondria, confirmed an increased mitochondrial localization of Cx43 in the heart of DOXO-treated mice (Figure 19).

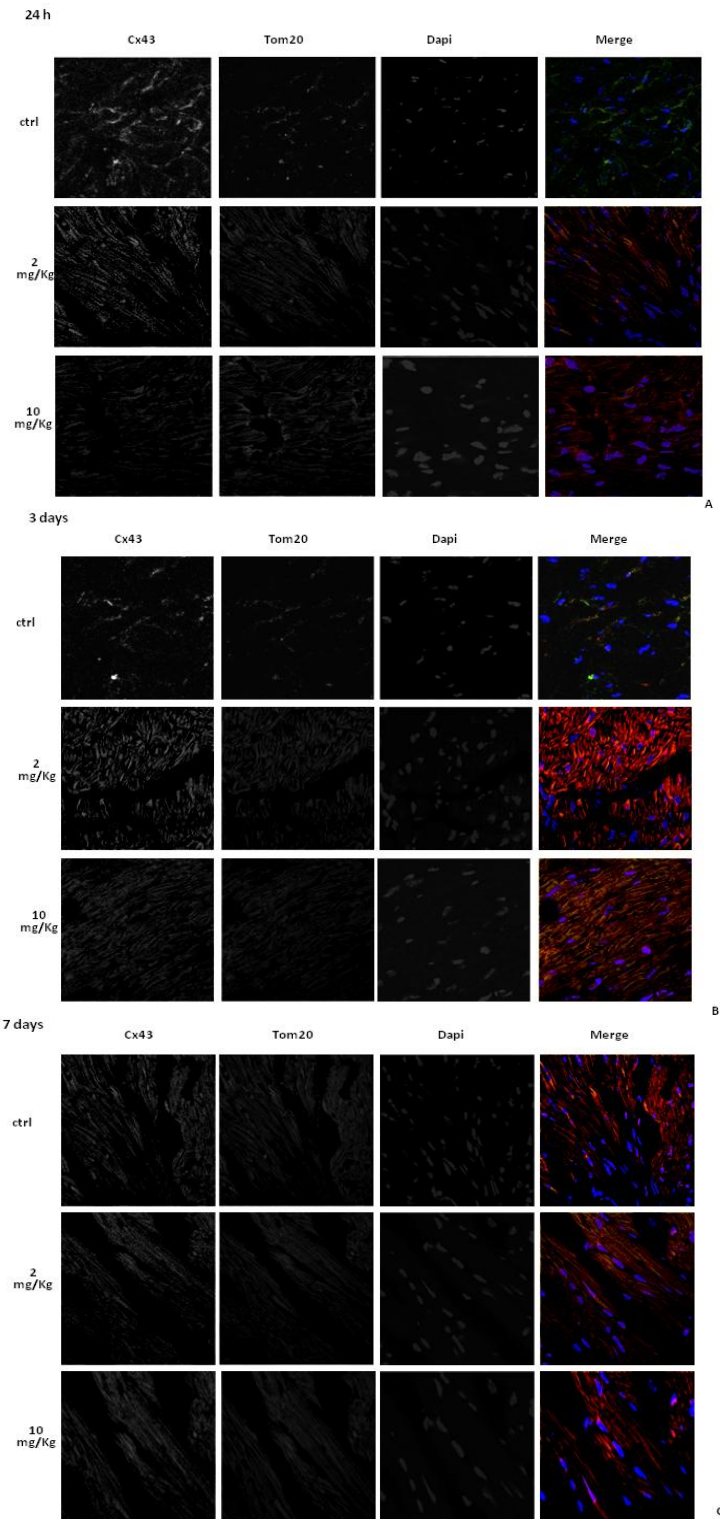


Figure 19 . Effect of DOXO (2 and 10 mg/kg; i.p.) on Cx43 localization in heart of C57BL/6j mice which received a single administration (1st group), two administrations (2nd group), or three administrations (3rd group). Frozen myocardial tissue sections were stained with Anti-Cx43 (green), TOM20 (red) and nucleus with DAPI (blue) and were determined by Immunofluorescence assay at confocal microscopy for mCx43 localization. Scale bar 10µm.

2.4 Discussion

DOXO is one of the most widely used and successful antitumor drugs, but its cumulative and dose-dependent cardiotoxicity limits its clinical application [Zhang et al., 2009]. Mechanisms of DOXO-induced cardiotoxicity are very complex and remain elusive. They include a rearrangement of GJs, responsible for the cell-to-cell communication, leading to mitochondrial injury and promoting myocardial cell apoptosis [Singale et al., 2000; Nakamura et al., 2000], with an alteration of calcium homeostasis [Severs et al., 2008]. Many studies report the long-term effects of DOXO while the effects of short-term treatment are not well elucidated. Doses of DOXO administered are 2 and 10 mg/kg and are the lowest doses reported in literature [Xujie et al., 2012; Wided et al., 2014]. Recently, we have demonstrated that the damage caused by DOXO on cardiac functions is immediate after drug administration in a short-time model of DOXO induced-cardiomyopathy in vivo [Pecoraro et al., 2016]. Furthermore the echocardiography showed in DOXO-treated mice a decreased Ejection Fraction (EF) and Fractiona Shortening (FS) compared with control mice, and an increased Left Ventricular End-Systolic Diameter (LVESD). These data suggest that the doses used in our experimental model are sufficient to induce clear signs of cardiac dysfunction. It is well known that contraction–relaxation cycle of the heart is

regulated by the sequential rise and fall of the cytosolic calcium concentration [Bers et al., 1997]. In our experimental model, we observed a significant dysfunction in Ca^{2+} homeostasis in DOXO-treated mice, as demonstrated by means of FURA 2-AM. In line with earlier reports [Periasamy et al., 2008], Western blot analysis showed a significant decrease of SERCAII expression in the heart of DOXO-treated mice, confirming the central role of SERCAII in maintaining intracellular calcium homeostasis in the heart [Mattila et al., 2016]. Moreover, our results showed a significant increased expression of PLB, a protein expressed in the sarcoplasmic reticulum membrane with inhibitory effects on SERCAII, in DOXO-treated mice, with a further alteration of cytosolic Ca^{2+} content. Recent evidence points to a role of Cx43 on intercellular communication and on homeostasis of Ca^{2+} and K^{+} [Azarashvili et al., 2011]. In fact, abnormal expression of Cx43, the main GJ's protein in the heart, has been reported in several forms of cardiomyopathies: i.e., hypertrophic, dilated, and ischemic cardiomyopathy [Pecoraro et al., 2015 a]. Our data demonstrate that DOXO administration significantly reduces Cx43 expression and, at the same time, increases the expression of its form phosphorylated on Ser368. In particular, phosphorylation on Ser368 creates a “closed”, conformational state, blocking the cell-to-cell communication and the

propagation of harmful stimuli. Intracellular Ca^{2+} homeostasis is fine-tuned by the cyclical uptake and release by the different cellular compartments [Gadicherla et al., 2017]. Recent evidence points to a role of Cx43 in mitochondrial homeostasis of Ca^{2+} [Azarashvili et al., 2011; Boengler et al., 2013].

The increase of mCx43 in cardiomyocytes can be induced by various stimuli, such as cellular stress and ischemic preconditioning, but its functional relevance is still unclear. It has been postulated that mCx43 is part of multiprotein complex that somehow controls mitochondrial homeostasis and that it forms hemichannels that serve as a conduit for ion flux [Miro-Casas et al., 2009], like Ca^{2+} . Interaction between proteins involved in this multiprotein complex is reinforced by PKC that mediates phosphorylation of the Cx43 at Ser368 residue [Waza et al., 2009]. In our experimental model, we found a significant increase of mCx43 and of mCx43 phosphorylated on Ser368 expression. mCx43 protects cardiomyocytes by mitigating Ca^{2+} overload, mitochondrial permeability transition, and cell death [Gadicherla et al., 2017]. In agreement with this hypothesis, our data show that increased mCx43 and mCx43 phosphorylated on Ser368 expression is associated with a reduced accumulation of Ca^{2+} in the mitochondria.

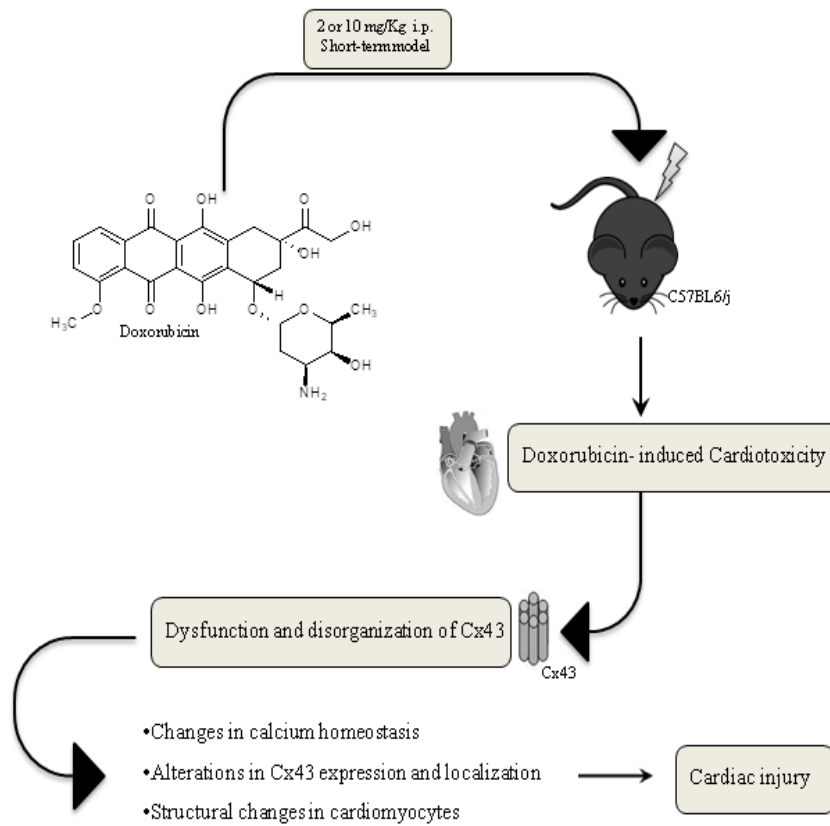


Figure 20: Cardiotoxic Effects of Short-Term DOXO administration. A short-term administration of DOXO is able to induce significant changes in Ca^{2+} homeostasis and alterations in Cx43 expression and localization. Indeed, each DOXO administration can induce structural changes in cardiomyocytes that ultimately lead to death of cardiomyocytes themselves.

Chapter III

Cardioprotective effects of Diazoxide in Doxorubicin- induced cardiotoxicity model

3.1 Introduction

Adenosine triphosphate-sensitive potassium channels (K_{ATP}) are abundantly expressed throughout the myocardium, however a definitive role in myocardial function has yet to be fully elucidated [Zhang et al., 2010]. K_{ATP} channels are formed as hetero-octamers of subunits that include 4 potassium inward rectifying (Kir) subunits and 4 regulatory subunits from the sulfonylurea receptor family (SUR1/2) (Nichols et al., 2013). Different combinations of Kir and SUR isoforms exist in different tissues, each with unique properties and function. The cardiac ventricular sarco K_{ATP} channel has been identified as comprising Kir6.2 and SUR2A as the predominant subunit combination [Kane et al., 2005]. K_{ATP} channels are ubiquitously expressed protein complexes hypothesized to provide a link between metabolic state and electrical excitability by virtue of their inhibition by ATP at normal physiological concentrations following direct binding of ATP to the Kir6 pore-forming subunit. In normal physiological conditions the channel is predominantly inhibited by ATP and are open during times of

stress, thus providing a “unique electrical transducer of the metabolic state of the cell” [Nichols et al., 2013; Noma et al., 1983]. Pharmacologic opening of K_{ATP} channels provides cardioprotection and mimics ischemic preconditioning in multiple animal models as well as in human myocytes [Henn et al., 2015]. Paradoxically, the cell surface (sarcolemmal) K_{ATP} channel has been implicated in myocyte swelling secondary to stress, and deletion of this channel provides resistance to myocyte swelling secondary to stress [Sellitto et al., 2011]. Cell surface K_{ATP} channels are composed of 4 pore-forming subunits (Kir6.2 or Kir6.1) and 4 of the ATP binding cassette family of membrane proteins (SUR1 or SUR2) [Flagg et al., 2010; Shyng et al., 1997].

An early hypothesis used to define the role of K_{ATP} channels suggested that during an ischemic insult, activation of the sarco K_{ATP} channel by a depletion of ATP and concurrent elevation in ADP, would cause a shortening of the cardiac action potential duration (APD) [Noma et al., 1983] and might lead to complete action potential failure, as the weakly rectifying K_{ATP} channel activity short-circuited the triggered depolarization. These actions could limit the rise in intracellular calcium and preserve cellular ATP.

Diazoxide (DZX), a specific opener of mitochondrial K_{ATP} channels, has been used in clinical practice since the early

1960's to treat severe non-malignant and malignant hypertension in hospitalized adults and acute severe hypertension in hospitalized children. DZX is also used to treat hypoglycaemia. The mechanisms of DZX's clinical action relate predominantly to the opening of pancreatic and smooth muscle K_{ATP} -channels [Coetzee et al., 2013]. Mitochondria are the major effectors of cardioprotection by mechanisms that open the mitochondrial K_{ATP} channel, including ischemic and pharmacological preconditioning [Garlid et al., 2013].

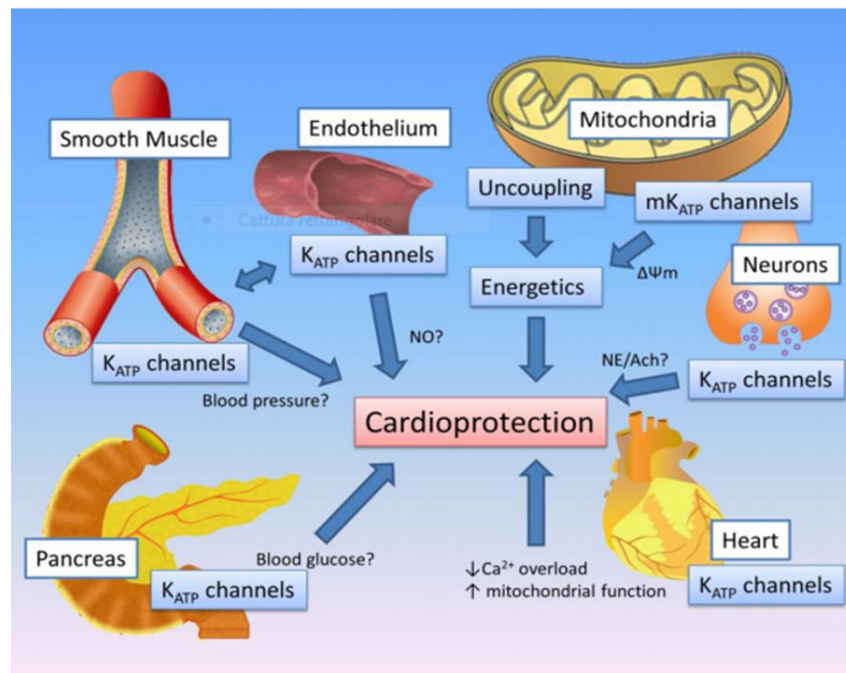


Figure 21: A cartoon summary of the main potential effectors of diazoxide, depicting some of the potential mechanisms by which they may contribute to cardioprotection. [Janjua et al., 2014]

The protective effect of DZX is equivalent to that of ischemic preconditioning, and DZX is often used as a pharmacological means to induce preconditioning [Coetze et al., 2013].

Pharmacological preconditioning, mimicking ischemic preconditioning, is suggested as an intervention to reduce DOXO cardiotoxicity [Kelishomi et al., 2008]. The drug has previously been described as an agent with a unique molecular target by opening of mitochondrial K_{ATP} -channels in cardioprotection. However, more recently a consensus seems to emerge that there are numerous effectors involved in the cardioprotective effects of DZX, and these effectors may synergistically contribute to its cardioprotective properties [Coetzee et al., 2013]. A possible effector involved in cardioprotection could be mCx43. So, we aimed to investigate if the pretreatment with DZX, could attenuate DOXO-induced cardiotoxicity in a short-time mice model.

3.2 Materials and Methods

3.2.1 Materials

DOXO was purchased from Baxter manufacturing S.p.a. (Officina di Sesto Fiorentino, Florence, Italy). Where not indicated otherwise, antibodies used were purchased from Santa Cruz Biotechnology (DBA, Milan, Italy), and all other products were purchased from Sigma (Milan, Italy).

3.2.2 Animals

Six week old female C57BL/6j (weighting 20–22 g) were purchased from Charles River (Lecco, Italy). All experimental procedures that involve animals have been conducted in agreement with the Italian and European Community Council for Animal Care (DL. no. 26/2014 protocol number of Ministerial approval DGSAF 13788-A 02/07/2015) and in accordance with the guidelines of the Guide for the Care and Use of Laboratory Animals of the National Institutes of Health.

3.2.3 Experimental Protocols

C57BL/6j mice were randomly divided in three groups (n = 12 for each experimental group). The doses used were 10 mg/kg [Pecoraro et al., 2017 b] for DOXO and 20mg/kg for DZX [Jazayeri et al., 2013].

First Group (24h):

- 3 mice received a single DOXO administration (10 mg/kg i.p.) and were sacrificed 24 hours after the treatment.
- 3 mice received a single DZX administration (20 mg/kg i.p.) and were sacrificed 24 hours after the treatment.
- 3 mice were pretreated with DZX (20 mg/kg i.p.) and then received a single DOXO (10 mg/kg i.p.) administration and were sacrificed 24 hours after the treatment.

Second Group(3 days):

- 3 mice received DOXO (10 mg/kg i.p.) every other day and were sacrificed 3 days after the treatment.
- 3 mice received DZX (20 mg/kg i.p.) every other day and were sacrificed 3 days after the treatment.
- 3 mice were pretreated with DZX (20 mg/kg i.p.) and then received DOXO (10 mg/kg i.p.) every other day and were sacrificed 3 days after the treatment.

Third Group (7 days):

- 3 mice received DOXO (10 mg/kg i.p.) every other day and were sacrificed 7 days after the treatment.
- 3 mice received DZX (20 mg/kg i.p.) every other day and were sacrificed 7 days after the treatment.
- 3 mice were pretreated with DZX (20 mg/kg i.p.) and then received DOXO (10 mg/kg i.p.) every other day and were sacrificed 7 days after the treatment.

Mice that received saline were used as control group.

Cardiac function was monitored echocardiographically at baseline and before sacrifice. At the end of each experimental time, heart samples were collected and prepared for molecular biological analyses.

3.2.4 Echocardiogram

Mice were lightly anesthetized with 1–1.5% of isoflurane in oxygen until the heart rate stabilized to 400–500 beats per minute. Echocardiography was performed using VEVO (VisualSonic, Toronto, (Canada) instrument. Ejection fraction (EF), Fractional shortening (FS), Left Ventricular End-Diastolic-Diameter (LVEDD), and Left Ventricular End-Systolic Diameter (LVESD) were calculated using the VEVO analysis software (Toronto, Canada).

3.2.5 Protein Extraction and Western Blot Analysis

Total proteins were extracted by homogenization of hearts with a dounce potter in lysis buffer (TRIS-HCl 50 mM, NaCl 500 mM, protease inhibitors, PMSF 0.25 μ M, NaF 50 mM, Na₃VO₄ 0.2 mM). Protein concentrations were determined with the Bio-Rad protein assay (BIO-RAD, Milan, Italy). Equal amounts of protein (50 μ g) were loaded into an acrylamide gel and separated by SDS-PAGE under denaturing conditions. Blots were incubated with primary antibody anti-Cx43 (Sigma, 1:8000), anti-pCx43 phosphorylate on Ser368 (Santa Cruz, 1:250), anti-sarco/endoplasmic reticulum Ca²⁺-ATP_{ase} (SERCAII; Santa Cruz, 1:250), anti-phospholamban (PLB; Santa Cruz, 1:250), or anti-glyceraldehyde 3-phosphate dehydrogenase (GAPDH; Santa Cruz, 1:1000, used as loading control) overnight at 4 °C. After incubation period with the primary antibodies, blots were washed in PBS 0.1% Tween. The appropriate secondary antibody—anti-rabbit, anti-mouse, or anti-goat (each diluted 1:4000) was added and allowed in incubation for 1 h at room temperature. Immunoreactive protein bands were detected by chemiluminescence using enhanced chemiluminescence reagents (ECL) in LAS 4000 (GE Healthcare, Björkgatan, Sweden).

3.2.6 Mitochondrial Protein Extraction and Western Blot Analysis for Mitochondrial Cx43 and pCx43

Mitochondrial proteins were extracted from homogenized hearts with a dounce potter in lysis buffer (sucrose 250 mM, K⁺ Hepes pH 7.5 20 mM, KCl 10 mM, MgCl₂ 1.5 mM, EDTA 0.1 mM, EGTA 1 mM, protease inhibitors, NaF 50 mM, Na₃VO₄ 0.2 mM, PMSF 100 μM, DTT 1 mM, digitonin 0.025%) as reported in chapter II. The protein yield was quantified with the Bio-Rad protein assay (BIO-RAD, Milan, Italy). Western blot analysis for Cx43 or pCx43 was performed as described above. Primary antibody anti-TOM20 (Santa Cruz) was used as loading control. In order to verify the purity of mitochondrial protein extraction, a Western blot analysis was performed to evaluate the presence of proteins expressed only in the mitochondria (ox-Phos Complex II, Abcam, 1:7000) and the absence of proteins expressed in other cellular compartments (Na⁺/K⁺ ATP_{ase}, Abcam, 1:3000) [Boengler et al., 2005].

3.2.7 Primary Cardiomyocytes Isolation and Measurement of Intracellular Ca²⁺ Signaling

Intracellular Ca²⁺ concentrations were measured in primary cardiomyocytes, isolated from hearts of mice treated as described above and from heart of control mice. Hearts were washed with HBSS 0.1 mM Ca²⁺ (140 mM NaCl, 5.4 mM KCl,

0.44 mM KH_2PO_4 , 0.42 mM Na_2HPO_4 , 4.17 mM NaHCO_3 , 26 mM CaNa-EDTA , 0.10 mM $\text{CaCl}_2 \cdot \text{H}_2\text{O}$, 5.0 mM HEPES and 5.5 mM dextrose). Next, hearts were cut in 1–2 mm sections and incubated at 37 °C in HBSS 0.1 mM Ca^{2+} containing albumin 10 mg/mL, trypsin inhibitor 1 mg/mL, taurine 5 mM, dithiothreitol 0.4 mg/mL, collagenase II 0.6 mg/mL, and papain 0.6 mg/mL for 75 min. After the incubation period, tissue fragments were removed by filtering the suspension with a 0.70 μ filter. Filtrate was centrifuged to collect the cardiomyocytes. Primary cardiomyocytes were loaded with the ratiometric fluorescent indicator dye FURA2-AM (5 μ M, 45 min, 37 °C) at a cell density of 3×10^4 cells/mL in HBSS 0.1 mM Ca^{2+} . FURA2-AM excess was removed by washing the cells with HBSS and cardiomyocytes were then transferred to a spectrofluorimeter (Perkin-Elmer LS-50). As reported for FURA2-AM, the excitation wavelength was alternated between 340 and 380 nm, and the emission wavelength was 515 nm. The basal F340/F380 ratio was recorded and then treatment with ionomycin (1 μ M), a calcium ionophore; thapsigargin (1 μ M), an inhibitor of sarco(endo) plasmic reticulum; or carbonyl cyanide p-trifluoromethoxyphenylhydrazone (FCCP; 50 nM), a mitochondrial calcium depletory, was added into the cuvette in Ca^{2+} -free HBSS and F340/F380 ratio was recorded 5 min after each stimulus induced. The ratio of fluorescence intensity of

340/380 nm (F340/F380) is strictly related to intracellular free $[Ca^{2+}]$ [Popolo et al., 2011]. Results are expressed as delta increase of F340/F380, calculated as F340/F380 stimulus - F340/F380 basal.

3.2.8 Immunohistochemical Analysis

For immunohistochemical analyses, frozen cardiac tissues were embedded in OCT compound (Bio-Optica, Milan, Italy). Sections (7 μ m) were incubated with mouse anti-Cx43 and rabbit anti-TOM20 for 2 h at room temperature. Then the slides were washed three times with PBS and incubated with secondary antibodies (FITC-conjugated anti mouse IgG and Texas red-conjugated anti rabbit IgG) for 1 h. DAPI was used to mark the nuclei.

After mounting, coverslips were examined by using a Laser Confocal Microscope (Leica TCS SP5, Wetzlar, Germany).

3.2.9 Statistical Analysis

Data are reported as the mean \pm standard error mean (S.E.M.) of at least three independent experiments. Statistical differences were assessed with Student's t-test. p-values of less than 0.05 was considered significant.

3.3 Results

3.3.1 Cardiac Functions

Mice were subjected to echocardiography at baseline and before the sacrifice to analyze the main parameters of cardiac function. As reported in Table 2, DOXO administration affects Ejection fraction (EF), Fractional shortening (FS), Left Ventricular End-Diastolic-Diameter (LVEDD), and Left Ventricular End-Systolic Diameter (LVESD) in mice after a single injection of DOXO. Indeed, compared with control mice, DOXO-treated mice exhibited decreased cardiac systolic function as measured by Ejection fraction (EF) and Fractional shortening (FS), and consequently increased Left Ventricular End-Diastolic-Diameter (LVEDD) and Left Ventricular End-Systolic Diameter (LVESD). In contrast, DZX increases cardiac function.

		Control	DOXO	DZX	DZX+DOXO
		24 hours	LVEDD	3.97 ± 0.11	4.09 ± 0.1
LVESD	2.62 ± 0.17		3,00 ± 0.06*	2.8 ± 0.40	2.67 ± 0.146
%EF	62.17 ± 4.1		52.7 ± 1,38**	53.0 ± 5.0	54.25 ± 1.8#
% FS	30.41 ± 0.72		26,6 ± 0.92*	27.0 ± 3.000	27.5 ± 0.936#
		Control	DOXO	DZX	DZX+DOXO
		3 days	LVEDD	3.940 ± 0.050	3.96 ± 0.06
LVESD	2.780 ± 0.054		2.90 ± 0.056*	2.70 ± 0.400	2.823 ± 0.107
%EF	57.20 ± 1.25		53.73 ± 1.61*	70.0 ± 1.000	50.500 ± 2.217
% FS	30.410 ± 0.850		27.43 ± 1.02*	39.5 ± 0.500	25.000 ± 0.354#
		Control	DOXO	DZX	DZX+DOXO
		7 days	LVEDD	3.860 ± 0.040	3.96±0.055*
LVESD	2.730 ± 0.150		2.9±0.14	2.350 ± 0.350	2.553 ± 0.135
%EF	59.000 ± 4.170		50.49±4.79**	63.0 ± 2.000	57.00± 2.606#
% FS	31.760 ± 1.680		25.39±3.02*	32.00 ± 2.000	29.000 ± 1.517#

Table 2: Effect of DOXO (10 mg/kg; i.p.) or DZX (20 mg/kg; i.p.) or combined DZX+DOXO treatment on Ejection Fraction (% EF), Fraction Shortening (% FS), Left Ventricular End-Diastolic Diameter (LVEDD) and on Left Ventricular End-Systolic Diameter (LVESD), after a single administration (1th group), two administrations (2nd group), or three administrations (3rd group). Results were expressed as mean ± S.E.M. from 12 mice/group.

3.3.2 Diazoxide Administration Alters Calcium Homeostasis

In order to evaluate the effects of DOXO, DZX or combined DZX+DOXO treatment on intracellular Ca^{2+} levels in our experimental model, primary cardiomyocytes from hearts of treated mice and from control mice were isolated and loaded with the fluorescent dye FURA2-AM in Ca^{2+} -free incubation medium (containing 0.5 mM EGTA).

Our data demonstrated that DZX-pretreatment significantly affected Calcium homeostasis. In fact, as indicated in Figure 22A and previously reported in Chapter II, DOXO

administration induced alterations in Ca^{2+} homeostasis by increasing intracellular free Ca^{2+} levels. Furthermore, as reported in Figure 22B and 22C, delta increase induced by both reticular ionophore (thapsigargin) and mitochondrial depletor (FCCP) in cardiomyocytes of DOXO-treated mice were significantly ($p < 0.05$) lower than those of control mice, indicating higher basal levels of Ca^{2+} . On the contrary, in primary cardiomyocytes of DZX+DOXO co-treated mice, reticular and mitochondrial Ca^{2+} levels was comparable to those of control mice.

SERCAII (Smooth Endoplasmic Reticulum Calcium ATP-Ase) protein is a Ca-dependent ATPasic pump that regulates the turnover of Ca^{2+} ions in the intracellular environment, between the sarcoplasmic reticulum and the cytosol, and its activation involves the reuptake of Ca^{2+} in the sarcoplasmic reticulum. The activity of SERCAII is, in turn, regulated by the PLB polymeric protein, which inhibits SERCAII depending on the degree of phosphorylation of the individual monomers of PLB [Periasamy et al., 2007]. The Western Blot analysis on heart homogenates shows, as reported in Figure 22D, that in the hearts of DOXO-treated mice, SERCAII levels are reduced compared to the hearts of control animals. In contrast, DZX promotes the expression of SERCAII, in fact the expression of this protein increase significantly at all experimental times. The expression

of PLB in the heart of DOXO-treated mice is significantly ($p < 0.05$) higher than control mice. In contrast, DZX pre-treatment results in a progressive reduction of PLB expression (Figure 22E).

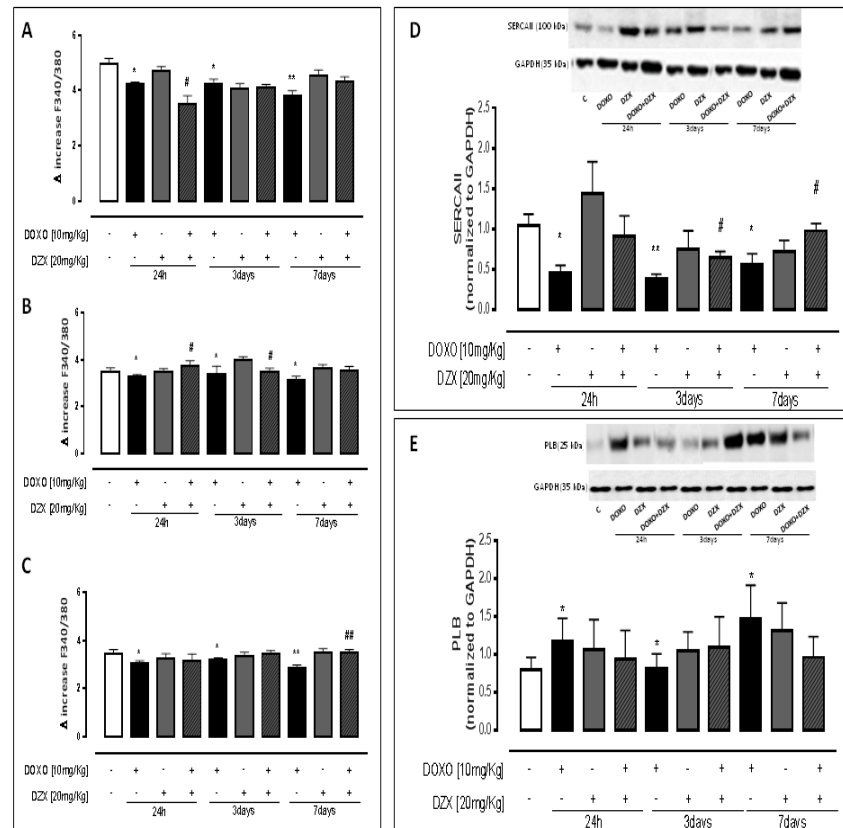


Figure 22: Effect of DOXO (10 mg/kg; i.p.) or DZX (20 mg/kg; i.p.) or combined DZX+DOXO treatment on calcium homeostasis. Mice received a single administration (1th group), two administrations (2nd group), or three administrations (3rd group) of DOXO (10 mg/kg; i.p.) or DZX (20 mg/kg; i.p.) or combined DZX+DOXO treatment and primary cardiomyocytes were isolated by enzymatic digestion. Intracellular calcium content in cells suspension was evaluated by using ionomycin (1 μ M) (A); reticulum calcium content was evaluated by means of thapsygargin (100 nM) (B) and mitochondrial calcium content was evaluated by using FCCP (50 nM) (C). Results were expressed as mean \pm S.E.M. of delta (δ) increase of FURA-2 AM ratio fluorescence (340/380 nm) from at least three independent experiments each performed in duplicate. Data were analyzed by Student's t-test. * $p < 0.05$, and ** $p < 0.005$ vs. control; # $p < 0.05$ and ## $p < 0.005$ DZX+DOXO vs DOXO. Effect of DOXO or DZX or combined DZX+DOXO treatment on SERCA II (D) and PLB (E) expression. Mice received a single administration (1th group), two administrations (2nd group), or three administrations (3rd group) of DOXO (10 mg/kg; i.p.) or DZX (20 mg/kg; i.p.) or combined DZX+DOXO treatment and SERCA II and PLB expressions were detected by Western blot analysis into tissue homogenates from mice; GAPDH protein expression was used as loading control. Values were expressed as mean \pm S.E.M. from at least three independent experiments each performed in duplicate. Data were analyzed by Student's t-test. * $p < 0.05$ and ** $p < 0.005$ vs. control; # $p < 0.05$ DZX+DOXO vs DOXO

3.3.3 Diazoxide Administration Affects Cx43 and pCx43 expression and localization

As depicted in Figure 23A, DOXO-treatment induces a decrease of total Cx43 expression also evident in mice that received a single DOXO administration. Western blot analysis performed on heart lysates of DOXO-treated mice confirmed that, compared to control mice, Cx43 expression was significantly ($p < 0.05$) reduced. On the contrary, Cx43 expression is higher in the heart of mice treated with DZX alone. DZX+DOXO co-treatment increases the expression of Cx43 compared to DOXO-treated mice. In fact, in the heart of DZX+DOXO co-treated mice the expression levels of Cx43 are comparable to those of control mice.

Connexin phosphorylation plays an important role in regulating biological function [Hood et al., 2017]. Western blot analysis showed a significant ($p < 0.05$) increase in Cx43 phosphorylated on Ser368 expression in DOXO-treated mice (Figure 23B) after 7 days of treatment. DZX+DOXO co-treatment defines a significant ($p < 0.001$) reduction of pCx43 compared to DOXO-treated mice. In fact, no significant differences are observed between DZX+DOXO co-treated mice and control mice.

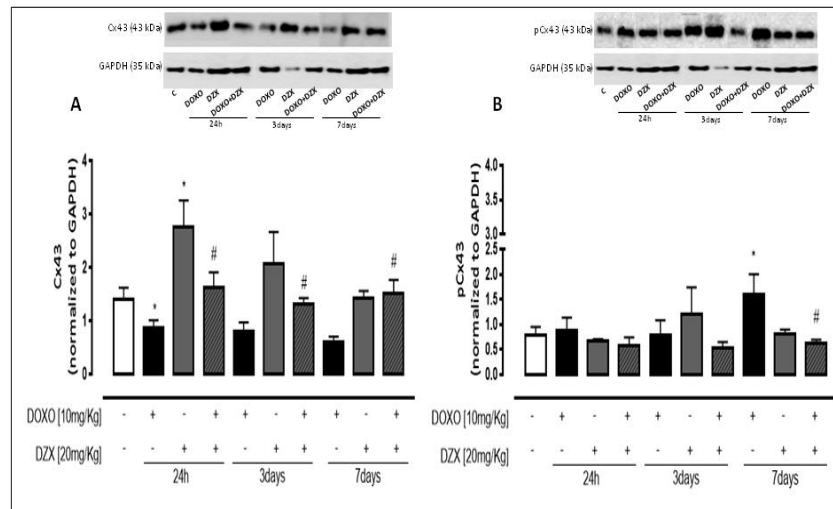


Figure 23: Effect of DOXO or DZX or combined DZX+DOXO treatment on Cx43 (A) and pCx43 (B) expression. Mice received a single administration (1th group), two administrations (2nd group), or three administrations (3rd group) of DOXO (10 mg/kg; i.p.) or DZX (20 mg/kg; i.p.) or combined DZX+DOXO treatment and Cx43 and pCx43 expressions were detected by Western blot analysis into tissue homogenates from mice; GAPDH protein expression was used as loading control. Values were expressed as mean \pm S.E.M. from at least three independent experiments each performed in duplicate. Data were analyzed by Student's t-test. * $p < 0.05$ vs. control; # $p < 0.05$ DZX+DOXO vs DOXO

3.3.4 Diazoxide Administration affects mitochondrial Cx43 and pCx43 expression

Western blot analysis performed on mitochondrial lysates from hearts of DOXO-treated mice show a significant ($p < 0.05$) increase of mCx43 at all experimental times. In the hearts of DZX+DOXO co-treated mice we observed a time-dependent increase of mCx43 expression (Figure 24A).

Regarding the expression levels of mCx43 phosphorylated on Ser 368 (Figure 24B) we observed an increase in the heart of DOXO-treated mice. It is to note that in the heart of DZX+DOXO co-treated mice mCx43 phosphorylated levels was

significantly higher than those of DOXO-treated mice, but a trend to reduction was observed through the time.

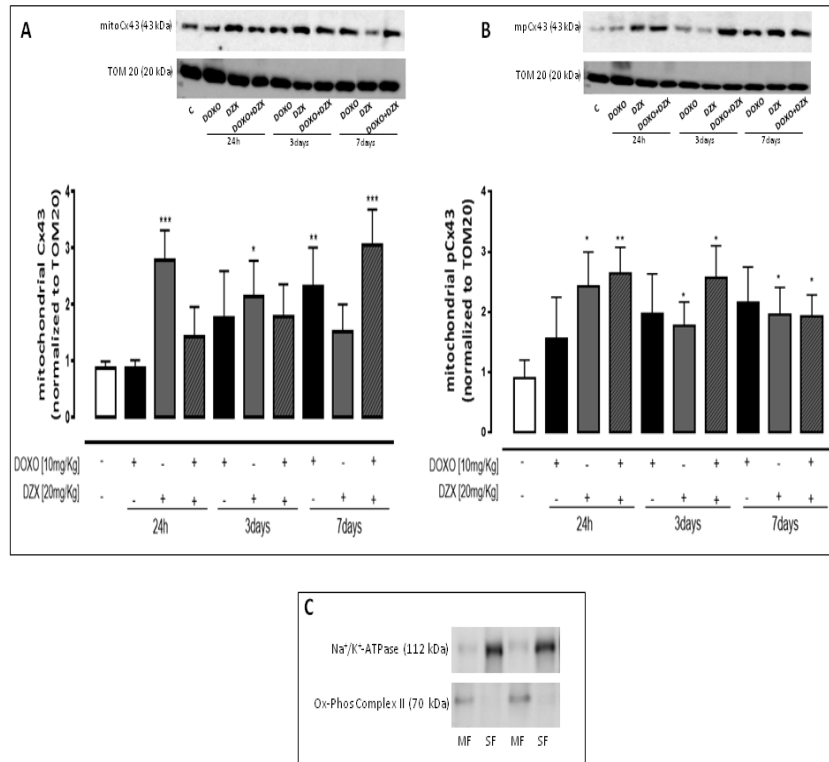


Figure 24: Effect of DOXO or DZX or combined DZX+DOXO treatment on mitochondrial Cx43 (A) and mCx43 phosphorylated (B) expression. Mice received a single administration (1th group), two administrations (2nd group), or three administrations (3rd group) of DOXO (10 mg/kg; i.p.) or DZX (20 mg/kg; i.p.) or combined DZX+DOXO treatment and mCx43 and mCx43 phosphorylated (mpCx43) expressions were detected by Western blot analysis into tissue homogenates from mice; TOM20 protein expression was used as loading control. Values were expressed as mean \pm S.E.M. from at least three independent experiments each performed in duplicate. Data were analyzed by Student's t-test. *p<0.05, **p<0.005 and ***p<0.001 vs. control. Representative Western blots of Na⁺/K⁺ATPase and Ox-Phos Complex II were used as markers of sarcolemma (SF) and mitochondria (MF), respectively, to demonstrate the purity of the mitochondrial extracts (C).

Immunofluorescence analysis performed on heart sections double-stained for Cx43 and TOM20, as a marker of mitochondria, confirmed an increased mitochondrial localization of Cx43 in the hearts of DZX+DOXO co-treated mice (Figure 25).

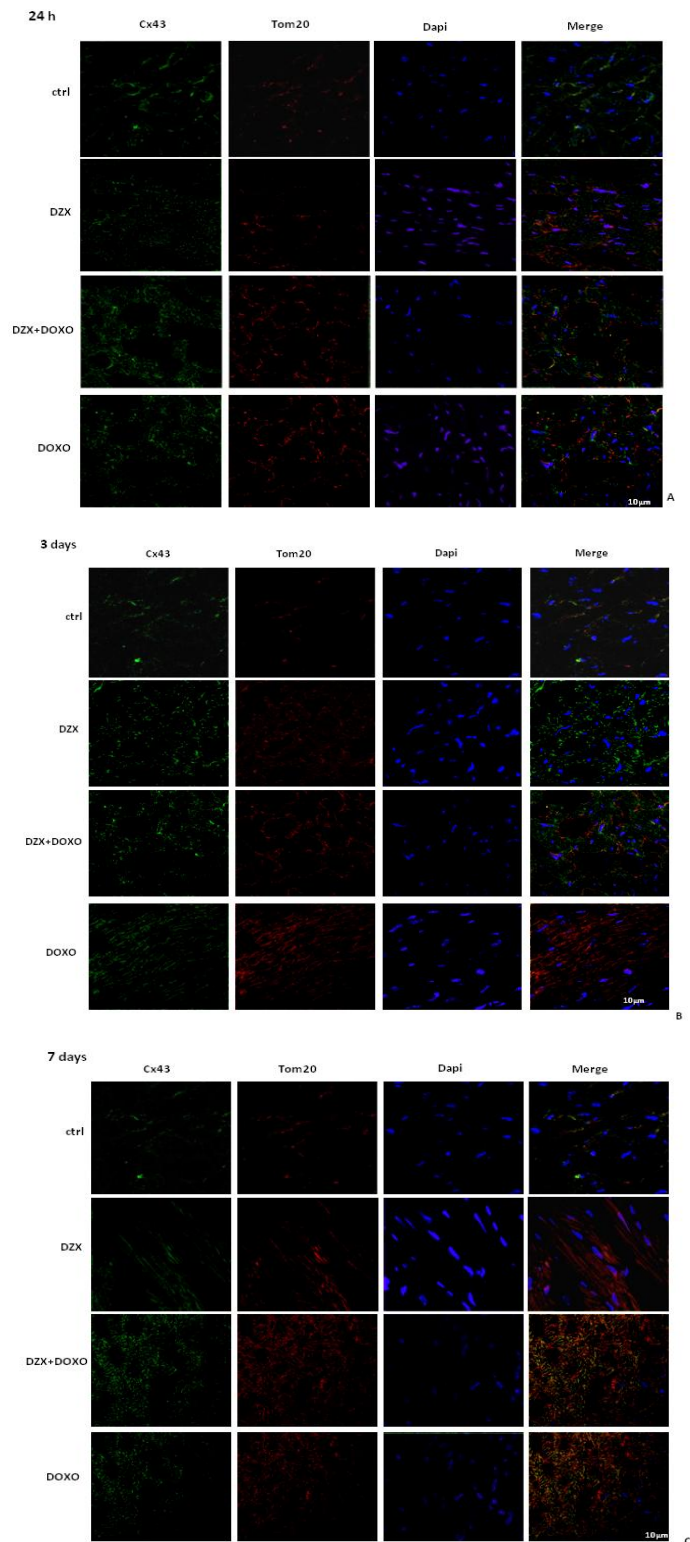


Figure 25. Effect of DOXO or DZX or combined DZX+DOXO treatment on Cx43 localization in heart of C57BL/6j mice which received a single administration (1st group), two administrations (2nd group), or three administrations (3rd group). Frozen myocardial tissue sections were stained with Anti-Cx43 (green), TOM20 (red) and nucleus with DAPI (blue) and were determined by Immunofluorescence assay at confocal microscopy for mCx43 localization. Scale bar 10 μ m.

3.4 Discussion

Chemotherapy with DOXO is limited by cardiotoxicity. Free radical generation and mitochondrial dysfunction are thought to contribute to DOXO-induced cardiac failure. In this study we wanted to investigate if opening of K_{ATP} -channels by Diazoxide (DZX) is protective against DOXO-cardiotoxicity, in a short-term model of DOXO-induced cardiomyopathy in mice.

In Chapter II we have shown that even a short-term model administration of DOXO is able to induce significant changes in calcium homeostasis and alterations in Cx43 expression and localization. Here, we focused on how the pretreatment with DZX attenuates DOXO-induced cardiac dysfunction in this model.

The DZX tries to restore the major cardiac parameters altered by treatment with DOXO, Ejection fraction (EF), Fractional shortening (FS), Left Ventricular End-Diastolic-Diameter (LVEDD), and Left Ventricular End-Systolic Diameter (LVESD), as observed with echocardiography in our experimental model. The heart rhythm is guaranteed by tight regulation of Ca^{2+} signalling. In Chapter II we observed a significant dysfunction in Ca^{2+} homeostasis in DOXO-treated mice.

Here, we demonstrated, by means of FURA-2AM, that the pretreatment with DZX keeps mitochondrial calcium levels

significantly higher than DOXO alone at all experimental times. Moreover, as demonstrated by Western blot analysis, the improvement of Ca^{2+} homeostasis, following pretreatment with DZX, was evidenced by the increase in SERCAII levels and a simultaneous progressive reduction in PLB expression.

Since Gadicherla and collaborators [2017] underline the strong link between mitochondrial calcium homeostasis and Cx43, we wanted to see the fate of Cx43 following the pretreatment of DZX in our experimental model.

As shown in the Chapter II, several forms of DOXO-induced cardiomyotoxicity are also characterized by redistribution of Cx43 expression in the heart. Moreover, its phosphorylation on Ser368, modulates the conductivity of the GJs [Lampe et al., 2000], blocking the chemical coupling. This mechanism is considered a “defense” from the propagation of injurious stimuli. Here we show that the pretreatment with DZX restores the expression levels of Cx43 and of its phosphorylated form.

Many studies report that DZX is able to induce translocation of PKC- ϵ from the cytosol to mitochondria in H9c2 cells, and, also, to induce its activation. The DZX-induced PKC- ϵ activation implies several cardioprotective properties [Coetzee et al., 2013; Kim, et al., 2006]. In human cardiomyocytes, PKC- ϵ is suspected to stabilize mitochondria, interacting with several targets [Barnett et al., 2008], such as Cx43 [Lia et al., 2013;

Lampe and Lau, 2000]. On the basis of our data, we hypothesized that in our experimental model, DZX pretreatment could form complexes with mCx43 and promote its phosphorylation at serine (Ser) 368 [Lia et al., 2013; Lampe and Lau, 2000], thus inducing the closure of hemichannels. In fact, data obtained by Western blot analysis showed an increase of mCx43 expression in all experimental conditions. Furthermore, we observed that DZX-pretreatment induces a significant increase of Cx43 phosphorylated expression on mitochondria compared to DOXO-treated mice. So we hypothesized that DZX promotes the closure of the hemichannels thus providing the storage of the Ca^{2+} in the mitochondria. In fact, as also discussed in the chapter I, the increased mitochondrial calcium uptake and storage capacity helps to delay a rise in cytosolic calcium levels which are more dangerous for cell viability. In fact, under high intracellular Ca^{2+} conditions, mitochondria may function as a buffer to control cytosolic Ca^{2+} concentrations, thus delaying cell death.

In conclusion, our data demonstrate that DZX represents a promising protective intervention to reduce the damage induced by DOXO. The cardioprotective effects of DZX are well documented. Here we reported that also Cx43 could be involved in these effects. In fact, the increase of Cx43 could be responsible for the improvement of cardiac functions observed

in DZX pre-treated mice, while the increased expression of mCx43 could be involved in the reduction of intracellular free- Ca^{2+} levels.

GENERAL CONCLUSION

Cx43 has multiple cellular locations and functions and changes in its expression and/or its channel and non-channel activities contribute to several cardiovascular pathologies (heart irreversible injury, arrhythmias). More research is needed to understand the pathophysiological alterations in Cx43 and to develop potential selective pharmacological approaches to reverse these effects. Therefore, in this doctoral project we investigated the involvement of Cx43, and in particular the crucial role of mCx43, in different cardiomyopathies models.

In an *in vitro* model of chemical hypoxia induced by adding Cobalt Chloride on H9c2 cell, we demonstrated that mCx43 plays a crucial role in cytoprotection by regulating calcium overload, mitochondrial ROS production, and mitochondrial membrane depolarization, consequently reduction of the triggering apoptotic pathway.

Afterwards, in an *in vivo* DOXO-induced cardiotoxicity in a short-term mouse model we showed that the mCx43 protects cardiomyocytes by mitigating Ca^{2+} overload, balancing the alterations that trigger cardiac damage.

In the end we observed that the pretreatment with DZX, an opener of mitochondrial K_{ATP} -channels, represents a promising protective intervention against DOXO-induced cardiotoxicity, reducing the calcium homeostasis alteration and trying to restore

the major cardiac parameters altered by DOXO treatment. This is in agreement with our hypothesis that mCx43 and DZX are involved in the cardioprotection mechanism.

In conclusion, we identified the Cx43, in particular mCx43, as a new therapeutic target that might improve the treatment cardiovascular pathologies in the future.

REFERENCES

- Ammar** E.S.M., Said S.A., El-Damarawy S.L., Suddek G.M. Cardioprotective effect of grape-seed proanthocyanidins on doxorubicin-induced cardiac toxicity in rats. *Pharmaceut. Biol.* (2013); 51:339–44.
- Azarashvili** T., Baburina Y., Grachev D., Krestinina O., Evtodienko Y., Stricker R., Reiser G. Calcium-induced permeability transition in rat brain mitochondria is promoted by carbenoxolone through targeting connexin 43. *Am. J. Physiol. Cell. Physiol.* (2011); 300:C707–C720.
- Baines** C.P. The mitochondrial permeability transition pore as a target of cardioprotective signaling. *Am. J. Physiol. Heart Circ. Physiol.* (2007); 293:H903–H904.
- Barnett** M., Lin D., Akoyev V., Willard L., Takemoto D. Protein Kinase C Epsilon Activates Lens Mitochondrial Cytochrome C Oxidase Subunit IV During Hypoxia. *Exp. Eye Res.* (2008); 86(2):226–234.
- Basheer** W.A., Shaw R.M. Connexin 43 and CaV1.2 Ion Channel Trafficking in Healthy and Diseased Myocardium. *Circ. Arrhythm. Electrophysiol.* (2016); 9(6):e001357.
- Beardslee** M.A., Laing J.G., Beyer E.C., Saffitz J.E. Rapid turnover of connexin 43 in the adult rat heart. *Circ. Res.* (1998); 83:629–635.

Beardslee M.A., Lerner, D.L., Tadros, P.N., Laing, J.G., Beyer, E.C., Yamada, K.A., Kleber, A.G., Schuessler, R.B., Saffitz, J.E. Dephosphorylation and Intracellular Redistribution of Ventricular Connexin43 During Electrical Uncoupling Induced by Ischemia. *Circulation Research* (2000);87:656-662.

Bers D.M. Ca transport during contraction and relaxation in mammalian ventricular muscle. *Basic Res Cardiol.* (1997); 92:1–10.

Bol M., Wang N., De Bock M., Wacquier B., Decrock E., Gadicherla A., Decaluwé K., Vanheel B., van Rijen H.V., Krysko D.V., Bultynck G., Dupont G., Van de Voorde J., Leybaert L. At the cross-point of connexins, calcium, and ATP: Blocking hemichannels inhibits vasoconstriction of rat small mesenteric arteries. *Cardiovasc. Res.* (2017); 113: 195–206.

Birgit E.J.T., Habo J.J., Marti F.A.B. Regulation of myocardial connexins during hypertrophic remodelling. *Eur.HeartJ.* (2004), 1979–1989.

Boengler K., Dodoni G., Rodriguez-Sinovas A., Cabestrero A., Ruiz-Meana M., Gres P., Konietzka I., Lopez-Iglesias C., Garcia-Dorado D., Di Lisa F., Heusch G., Schulz R. Connexin 43 in cardiomyocyte mitochondria and its increase by ischemic preconditioning. *Cardiovasc Res.* (2005); 67: 234–244.

Boengler K., Schulz R., Heusch G. Connexin43 signalling and cardioprotection. *Heart* (2006), 92: 1724–1727.

Boengler K., Ruiz-Meana M., Gent S., Ungefug E., Soetkamp D., Miro-Casas E., Cabestrero A., Fernandez-Sanz C., Semenzato M., Di Lisa F., Rohrbach S., Garcia-Dorado D., Heusch G., Schulz R. Mitochondrial connexin 43 impacts on respiratory complex I activity and mitochondrial oxygen consumption, *J Cell Mol Med.* (2012); 16: 1649–1655.

Boengler K., Ungefug E., Heusch G., Leybaert L., Schulz R. Connexin 43 impacts on mitochondrial potassium uptake. *Front. Pharmacol.* (2013); 4, 73.

Cabo C., Boyden P.A. Extracellular space attenuates the effect of gap junctional remodeling on wave propagation: a computational study. *Biophys J.* (2009); 96: 3092-101.

Cardinale D., Colombo A., Bacchiani G., et al. Early Detection of Anthracycline Cardiotoxicity and Improvement With Heart Failure Therapy. *Circulation* (2015); 131:1981-8.

Carvalho F.S., Burgeiro A., Garcia R., Moreno A.J., Carvalho R.A., Oliveira P.J. Doxorubicin-induced cardiotoxicity: From bioenergetic failure and cell death to cardiomyopathy. *Med Res Rev.* (2014); 34:106–35.

Chatterjee K., Zhang J., Honbo N., Karliner J.S. Doxorubicin Cardiomyopathy. *Cardiology* (2010), 115: 155–162.

Coetzee W.A. Multiplicity of effectors of the cardioprotective agent, diazoxide. *Pharmacol Therapeut.* (2013); 140(2):167–175.

Columbia University medical center. Hypertrophic Cardiomyopathy and Heart Failure. Department of Surgery (1999-2017).

Crimi G., Pica S., Raineri C., Bramucci E., De Ferrari G.M., Klersy C., Ferlini M., Marinoni B., Repetto A., Romeo M., Rosti V., Massa M., Raisaro A., Leonardi S., Rubartelli P., Oltrona Visconti L., Ferrario M. Remote ischemic post-conditioning of the lower limb during primary percutaneous coronary intervention safely reduces enzymatic infarct size in anterior myocardial infarction: A randomized controlled trial. *JACC Cardiovasc Interv.* (2013); 6: 1055-1063.

Dando I., Fiorini C., Pozza E.D., Padroni C., Costanzo C., Palmieri M., Donadelli M. UCP2 inhibition triggers ROS-dependent nuclear translocation of GAPDH and autophagic cell death in pancreatic adenocarcinoma cells. *Biochim. Biophys. Acta* (2013); 1833: 672–679.

Dazzi H., Kaufmann K., Follath F. Anthracycline-induced acute cardiotoxicity in adults treated for leukaemia. Analysis of the clinico-pathological aspects of documented acute anthracycline-induced cardiotoxicity in patients treated for acute leukaemia at the University Hospital of Zurich, Switzerland, between 1990 and 1996. *Ann Oncol* (2001); 12:963-6.

Decrock E., Vinken M., Bol M., D'Herde K., Rogiers V., Vandenaabeele P., Krysko D.V., Bultynck G., Leybaert L. Calcium and connexin-based intercellular communication, a deadly catch? *Cell Calcium* (2011); 50:310–321.

De Maio A., Vega V.L., Contreras J.E. Gap junctions, homeostasis, and injury. *J Cell Physiol.* (2002); 191(3):269–282.

Du Z.J., Cui G.Q., Zhang J., Liu X.M., Zhang Z.H., Jia Q., Ng J.C., Peng C., Bo C.X., Shao H. Inhibition of gap junction intercellular communication is involved in silica nanoparticles-induced H9c2 cardiomyocytes apoptosis via the mitochondrial pathway. *Int J Nanomedicine.* (2017); 12:2179-2188.

Feliksas F., Bukauskas. Molecular Organization, Gating, and Function of Gap Junction Channels. *Neuroscience.* (2013)

Ferrans V.J., Clark J.R., Zhang J., Yu Z.X., Herman E.H. Pathogenesis and prevention of doxorubicin cardiomyopathy. *Tsitologiya* (1997), 39: 928–936.

Flagg T.P., Enkvetchakul D., Koster J.C., Nichols C.G. Muscle K_{ATP} channels: recent insights to energy sensing and myoprotection. *Physiological Rev.* (2010); 90:799–829.

Fontes M.S., vanVeen T.A., deBakker J.M., vanRijen H.V. Functional consequences of abnormal Cx43 expression in the heart. *Biochim. Biophys. Acta* (2012); 1818: 2020–2029.

Fouad A.A., Yacoubi M.T. Mechanisms underlying the protective effect of eugenol in rats with acute doxorubicin cardiotoxicity. *Arch. Pharmaceut. Res.* (2011); 34:821–8.

Freireich E.J. The future of clinical cancer research in the next millennium. *Clin. Cancer Res.* (1997); 3: 2563–2570.

Gadicherla A.K., Wang N., Bulic M., Agullo-Pascual E., Lissoni A., De Smet M., Delmar M., Bultynck G., Krysko D.V., Camara A., Schlüter K., Schulz R, Kwok W., Leybaert L. Mitochondrial Cx43 hemichannels contribute to mitochondrial calcium entry and cell death in the heart. *Basic Res. Cardiol.* (2017); 112:27.

Garlid K.D., Dos Santos P., Xie Z.J., Costa A.D., Paucek P. Mitochondrial potassium transport: the role of the mitochondrial ATP-sensitive K^{+} channel in cardiac function and cardioprotection. *Biochim. Biophys. Acta* (2003), 1606(1–3):1–21.

Gewirtz D.A. A critical evaluation of the mechanisms of action proposed for the antitumor effects of the anthracycline antibiotics adriamycin and daunorubicin. *Biochem Pharmacol* (1999); 57: 727–741.

Ghigo A., Li M., Hirsch E. New signal transduction paradigms in anthracycline-induced cardiotoxicity. *Biochim Biophys Acta* (1983); 1916–1925.

Goldberg M.A., Dunning S.P., Bunn H.F. Regulation of the erythropoietin gene - evidence that the oxygen sensor is a heme protein. *Science* (1988); 242: 1412–1415.

Goodenough D.A., Paul D.L. Beyond the gap: functions of unpaired connexon channels. *Nat Rev Mol Cell Biol.* (2003); 4:285–294.

Goubaeva F., Mikami M., Giardina S., Ding B., Abe J., Yang J. Cardiac Mitochondrial Connexin 43 Regulates Apoptosis. *Biochem. Biophys. Res. Commun.* (2007); 352(1): 97–103.

Gunter T.E., Yule D.I., Gunter K.K., Eliseev R.A., Salter J.D. Calcium and mitochondria. *FEBS Lett.* (2004); 567:96–102.

Gutstein D.E., Morley G.E., Vaidya D., Liu F., Chen F.L., Stuhlmann H., Fishman G.I. Heterogeneous expression of gap junction channels in the heart leads to conduction defects and ventricular dysfunction. *Circulation.* (2001); 104:1194–1199.

Gutstein D.E., Morley G.E., Tamaddon H., Vaidya D., Schneider M.D., Chen J., Chien K.R., Stuhlmann H., Fishman G.I. Conduction slowing and sudden arrhythmic death in mice with cardiac-restricted inactivation of connexin43. *Circ. Res.* (2001 a); 88:333–339.

Gutstein D.E., Morley G.E., Fishman G.I. Conditional gene targeting of connexin43: exploring the consequences of gap junction remodeling in the heart. *Cell Commun Adhes.* (2001 b); 8:345–348.

Henn M.C., Janjua M.B., Zhang H., Kanter E.M., Makepeace C.M., Schuessler R.B., Nichols C.G., Lawton J.S. Diazoxide Cardioprotection Is Independent of Adenosine Triphosphate-Sensitive Potassium Channel Kir6.1 Subunit in Response to Stress. *J Am Coll Surg.* (2015), (2): 319–325.

Hrdina R., Gersl V., Klimtová I., Simůnek T., Machácková J., Adamcová M. Anthracycline-induced cardiotoxicity. *Acta Medica (Hradec Kralove)*, (2000); 43: 75-82.

Hood A.R., Ai X., Pogwizd S.M. Regulation of cardiac gap junctions by protein phosphatases. *J Mol Cell Cardiol.* (2017);107:52-57.

Jabr R.I., Hatch F.S., Salvage S.C., Orłowski A., Lampe P. D., Fry C.H. Regulation of gap junction conductance by calcineurin through Cx43 phosphorylation: implications for action potential conduction. *Pflugers Arch.* (2016); 468(11): 1945–1955.

Jain D., Ahmad T., Cairo M., Aronow W. Cardiotoxicity of cancer chemotherapy: identification, prevention and treatment. *Column in Hypertension, Ann Transl Med.* (2017); 5(17):348.

Janjua M.B., Makepeace C.M., Anastacio M.M., Schuessler R.B., Nichols C.G., Lawton J.S. Cardioprotective Benefits of Adenosine Triphosphate: Sensitive Potassium Channel Opener Diazoxide Are Lost with Administration after the Onset of Stress in Mouse and Human Myocytes. *J Am Coll Surg.* (2014);219(4):803-13.

Jazayeri A., Zolfaghari S., Ostadhadi S. Anticonvulsant effect of Diazoxide against Dichlorvos-induced seizures in mice. *Scientific World Journal*. (2013);697305.

Jeyaraman M.M., Srisakuldee W., Nickel B.E., Kardami E. Connexin43 phosphorylation and cytoprotection in the heart. *Biochim. Biophys. Acta* (2012); 1818: 2009–2013.

Jezek P., Olejar T., Smolkova K., Jezek J., Dlaskova A., Plecita-Hlavata L., Zelenka J., Spacek T., Engstova H., Pajuelo Reguera D., Jaburek M. Antioxidant and regulatory role of mitochondrial uncoupling protein UCP2 in pancreatic beta-cells. *Physiol. Res.* (2014); 63: S73–S91.

Jiang Z.H., Zhang T.T., Zhang J.F. Protective effects of fasudil hydrochloride post-conditioning on acute myocardial ischemia/reperfusion injury in rats. *Cardiol J.* (2013); 20: 197-202.

Johansen D., Cruciani V., Sundset R., Ytrehus K., Mikalsen, S. Ischemia Induces Closure of Gap Junctional Channels and Opening of Hemichannels in Heart-derived Cells and Tissue. *Cell Physiol Biochem.* (2011); 28:103-114.

Jung F., Weiland U., Johns R.A., Ihling C., Dimmeler S. “Chronic hypoxia induces apoptosis in cardiomyocytes: a possible role for Bcl 2-like Proteins”. *Biochemical and Biophysical Research Communications.* (2001); 286(2): 419–425.

Jung J.Y., Kim W.J. Involvement of mitochondrial- and Fas-mediated dual mechanism in CoCl₂-induced apoptosis of rat PC12 cells. *Neurosci. Lett.* (2004); 371: 85–90.

Kalvelyte A., Imbrasaite A., Bukauskiene A., Verselis V.K., Bukauskas F.F. Connexins and apoptotic transformation. *Biochem. Pharmacol.* (2003); 66: 1661–1672.

Kane G.C., Liu X.K., Yamada S., Olson T.M., Terzic A. Cardiac K_{ATP} channels in health and disease. *J Mol Cell Cardiol.* (2005); 38:937 – 43

Kardami E., Dang X., Iacobas D.A., Nickel B.E., Jeyaraman M., Srisakuldee W., Makazan J., Tanguy S., Spray D.C. The role of connexins in controlling cell growth and gene expression. *Prog Biophys Mol Biol.* (2007); 94: 245-264.

Kavazis A.N., Morton A.B., Hall S.E., Smuder A.J. Effects of doxorubicin on cardiac muscle subsarcolemmal and intermyofibrillar mitochondria. *Mitochondrion* (2016); 34:9-19

Kelishomi R.B., Ejtemaemehr S., Tavangar S.M., Rahimian R., Mobarakeh J.I., Dehpour A.R. Morphine is protective against doxorubicin-induced cardiotoxicity in rat. *Toxicology* (2008); 243 (1–2): 96–104.

Kim M.Y., Kim M.J., Yoon I.S., Ahn J.H., Lee S.H., Baik E.J., Moon C.H., Jung Y.S. Diazoxide acts more as a PKC-epsilon activator, and indirectly activates the mitochondrial K(ATP) channel conferring cardioprotection against hypoxic injury. *British Journal of Pharmacology*. (2006); 149:1059–1070.

Kleber A.G., Rudy Y. Basic mechanisms of cardiac impulse propagation and associated arrhythmias. *Physiol Rev*. (2004); 84:431–488.

Kristiań T., Siesjoń B.K. Calcium in ischemic cell death. *Stroke* (1998); 29:705–718.

Krysko D.V, Leybaert L., Vandenabeele P., D’Herde K. Gap junctions and the propagation of cell survival and cell death signals. *Apoptosis*. 2005; 10:459–469.

LadyofHats M.R. Connexon and connexin structure. *Wikipedia* (2006).

Lampe P.D., TenBroek E.M., Burt J.M., Kurata K.W., Johnson R.G., Lau A.F. Phosphorylation of connexin43 on serine368 by protein kinase C regulates gap junctional communication. *J Cell Biol*. (2000 a); 149:1503–1512.

Lampe P.D. and Lau A.F. Regulation of gap junctions by phosphorylation of connexins. *Arch. Biochem. Biophys*. (2000 b); 384: pp. 205-215.

Liao C.K., Cheng H.H., Wang S.D., Yeih D.F., Wang S.M. PKC ϵ mediates serine phosphorylation of connexin43 induced by lysophosphatidylcholine in neonatal rat cardiomyocytes. *Toxicology*. (2013); 314(1):11-21.

Lin J.H., Yang J., Liu S., Takano T., Wang X., Gao Q., Willecke K., Nedergaard M. Connexin mediates gap junction-independent resistance to cellular injury. *J Neurosci* (2003); 23:430–41.

Lipshultz S.E., Colan S.D., Gelber R.D., Perez-Atayde A.R., Sallan S.E., Sanders S.P. Late cardiac effects of doxorubicin therapy for acute lymphoblastic leukemia in childhood. *N Engl J Med*. (1991); 324:808-15.

Lipshultz S.E., Lipsitz S.R., Sallan S.E., Dalton V.M., Mone S.M., Gelber R.D., Colan S.D. Chronic progressive cardiac dysfunction years after doxorubicin therapy for childhood acute lymphoblastic leukemia. *J Clin Oncol*. (2005); 23:2629-36.

Liu Y., Nie H., Zhang K., Ma D., Yang G., Zheng Z., Liu K., Yu B., Zhai C., Yang S. A feedback regulatory loop between HIF-1 α and miR-21 in response to hypoxia in cardiomyocytes. *FEBS Lett*. (2014); 588(17): 3137-46.

Ma Y., Yang L., Ma J., Lu L., Wang X., Ren J., Yang J. Rutin attenuates doxorubicin-induced cardiotoxicity via regulating autophagy and apoptosis. *Biochim. Biophys. Acta* (2017); 1863: 1904–1911.

Mattila M., Koskenvuo J., Söderström, M., Eerola K., Savontaus M. Intramyocardial injection of SERCA2a-expressing lentivirus improves myocardial function in doxorubicin-induced heart failure. *J. Gene Med.* (2016); 18: 124–133.

Marquez-Rosado L., Solan J.L., Dunn C.A., Norris R.P., Lampe P.D. Connexin43 phosphorylation in brain, cardiac, endothelial and epithelial tissues. *Biochim Biophys Acta.* (2011); 1818(8):1985-92.

Martel C., Huynh le H., Garnier A., Ventura-Clapier R., Brenner C. Inhibition of the mitochondrial permeability transition for cytoprotection: direct versus indirect mechanisms. *Biochem. Res. Int.* (2012); 213403.

Medrano F.L., Munoz A.S., Sánchez V.S., Pérez-Herrero J.R.C. Cardiotoxicity of 5 fluorouracil: Ischemia or myocardial toxicity?. *Revista Clínica Española* (2001); 201: 106–107.

Menna P., Salvatorelli E., Minotti G. Cardiotoxicity of antitumor drugs. *Chem. Res. Toxicol.* (2008); 21: 978-89.

Miro-Casas E., Ruiz-Meana M., Agullo E., Stahlhofen S., Rodríguez-Sinovas A., Cabestrero A., Jorge I., Torre I., Vazquez J., Boengler K., Schulz R., Heusch G., Garcia-Dorado D. Connexin43 in cardiomyocyte mitochondria contributes to mitochondrial potassium uptake. *Cardiovasc. Res.* (2009); 83: 747–756.

Mykytenko J., Reeves J.G., Kin H., Wang N.P., Zatta A.J., Jiang R., Guyton R.A., Vinten-Johansen J., Zhao Z.Q. Persistent beneficial effect of postconditioning against infarct size: Role of mitochondrial K_{ATP} channels during reperfusion. *Basic Res Cardiol.* (2008); 103: 472-484.

Nakamura T., Ueda Y., Juan Y., Katsuda S., Takahashi H., Koh E: Fas-mediated apoptosis in adriamycin-induced cardiomyopathy in rats: In vivo study. *Circulation.* (2000); 102: 572-578.

Netter F. Acquired Heart Disease. *Cardiuvascular* (2015).

Nichols C.G. K_{ATP} channels as molecular sensors of cellular metabolism. *Nature.* (2006); 440:470–476.

Nichols C.G., Singh G.K., Grange D.K. K_{ATP} channels and cardiovascular disease: suddenly a syndrome. *Circ Res.* (2013); 112:1059–1072.

Noma A. ATP-regulated K^+ channels in cardiac muscle. *Nature.* (1983); 305:147–148.

Nordgren K.K., Wallace K.B. Keap1 redox-dependent regulation of doxorubicin-induced oxidative stress response in cardiac myoblasts. *Toxicol. Appl. Pharmacol.* (2014); 274: 107-16.

O' Connell J.L., Romano M.M., Campos Pulici E.C., Carvalho E.E., de Souza F.R., Tanaka D.M., Maciel B.C., Salgado H.C., Fazan-Júnior R., Rossi M.A., Simões M.V. Short-term and long-term models of doxorubicin-induced cardiomyopathy in rats: A comparison of functional and histopathological changes. *Exp. Toxicol. Pathol.* (2017); 69: 213–219.

Octavia Y. et al. Doxorubicin-induced cardiomyopathy: from molecular mechanisms to therapeutic strategies. *J Mol Cell Cardiol.* (2012); 52: 1213–1225.

Pecoraro M., Verrilli V., Pinto A., Popolo A. Role of connexin 43 in cardiovascular diseases. *Eur J Pharmacol.* (2015 a); 768:71-6.

Pecoraro M., Sorrentino R., Franceschelli S., Del Pizzo M., Pinto A., Popolo A. Doxorubicin-Mediated Cardiotoxicity: Role of Mitochondrial Connexin 43. *Cardiovasc. Toxicol.* (2015 b); 15: 366–376.

Pecoraro M., Del Pizzo M., Marzocco S., Sorrentino R., Ciccarelli M., Iaccarino G., Pinto A., Popolo A. Inflammatory mediators in a short-time mouse model of doxorubicin-induced cardiotoxicity. *Toxicol. Appl. Pharmacol.* (2016); 293: 44–52.

Pecoraro M., Pinto A., Popolo A. Inhibition of Connexin 43 translocation on mitochondria accelerates CoCl_2 -induced apoptotic response in a chemical model of hypoxia. *Toxicol In Vitro.* (2017 a); pii: S0887-2333(17)30354-5.

Pecoraro M.; Rodríguez-Sinovas A.; Marzocco S.; Ciccarelli M.; Iaccarino G.; Pinto A.; Popolo A. Cardiotoxic Effects of Short-Term Doxorubicin Administration: Involvement of Connexin 43 in Calcium Impairment. *Int. J. Mol. Sci.* (2017 b); 18(10): 2121.

Pennacchietti S., Michieli P., Galluzzo M., Mazzone M., Giordano S., Comoglio P.M. Hypoxia promotes invasive growth by transcriptional activation of the met protooncogene. *Cancer Cell.* (2003); 3: 347–361.

Periasamy M., Bhupathy P., Babu G.J. Regulation of sarcoplasmic reticulum Ca^{2+} ATP_{ase} pump expression and its relevance to cardiac muscle physiology and pathology. *Cardiovasc. Res.* (2008); 77: 265–273.

Popolo A., Piccinelli A.L., Morello S., Sorrentino R., Osmany C.R., Rastrelli L., Pinto A. Cytotoxic activity of nemorosone in human MCF-7 breast cancer cells. *Can. J. Physiol. Pharmacol.* (2011); 89: 50–57.

Prevedel L., Morocho C., Bennett M.V.L., Eugenin E.A. HIV-Associated Cardiovascular Disease: Role of Connexin 43 *Am J Pathol.* (2017); 187(9):1960-1970.

Reaume A.G., de Sousa P.A., Kulkarni S., Langille B.L., Zhu D., Davies T.C., Juneja S.C., Kidder G.M., Rossant J. Cardiac malformation in neonatal mice lacking connexin43. *Science.* (1995); 267:1831–1834.

Ren D., Zhu Q., Li J., Ha T., Wang X., Li Y. Overexpression of angiopoietin-1 reduces doxorubicin-induced apoptosis in cardiomyocytes. *J Biomed Res.* (2012); 26:432–8.

Revel J.P., Karnovsky M.J. Hexagonal array of subunits in intercellular junctions of the mouse heart and liver. *J Cell Biol.* (1967), 33:C7–C12.

Robert, J. Long-term and short-term models for studying anthracycline cardiotoxicity and protectors. *Cardiovasc. Toxicol.* (2007); 7: 135–139

Rodríguez-Sinovas A., Boengler K., Cabestrero A., Gres P., Morente M., Ruiz-Meana M., Konietzka I., Miro E., Totzeck A., Heusch G., Schulz R., Garcia-Dorado D. Translocation of connexin 43 to the inner mitochondrial membrane of cardiomyocytes through the heat shock protein 90-dependent TOM pathway and its importance for cardioprotection, *Circ. Res.* (2006); 99: 93–101.

Rodríguez-Sinovas A., Ruiz-Meana M., Denuc A., García-Dorado D. Mitochondrial Cx43, an important component of cardiac preconditioning. *Biochimica et Biophysica Acta* (2017); 1860(1):174-181.

Roger V.L., Go A.S., Lloyd-Jones D.M., Benjamin E.J., Berry J.D., Borden W.B., Bravata D.M., Dai S., Ford E.S., Fox C.S., Fullerton H.J., Gillespie C., Hailpern S.M., Heit J.A., Howard V.J., Kissela B.M., Kittner S.J., Lackland D.T., Lichtman J.H., Lisabeth L.D., Makuc D.M., Marcus G.M., Marelli A., Matchar D.B., Moy C.S., Mozaffarian D., Mussolino M.E., Nichol G., Paynter N.P., Soliman E.Z., Sorlie P.D., Sotoodehnia N., Turan T.N., Virani S.S., Wong N.D., Woo D., Turner M.B. American Heart Association Statistics Committee and Stroke Statistics Subcommittee. Heart disease and stroke statistics - 2012 update: A report from the American Heart Association. *Circulation* (2012); 125: e2-e220, 2012.

Rohr S. Role of gap junctions in the propagation of the cardiac action potential. *Cardiovasc Res.* (2004); 62:309–322.

Rosenthal N.N. A Guardian of the Heartbeat. *Engl J Med.* (2017); 377(1):84-86.

Ruiz-Meana M., Garcia-Dorado D., Lane S., Pina P., Inverte J., Mirabet M., Soler-Soler J. Persistence of gap junction communication during myocardial ischemia. *Am. J. Physiol. Heart Circ. Physiol.* (2001); 280: H2563-2571.

Ruiz-Meana M., Rodriguez-Sinovas A., Cabestrero A., Boengler K., Heusch G., Garcia-Dorado D. Mitochondrial connexin43 as a new player in the pathophysiology of myocardial ischaemia-reperfusion injury. *Cardiovasc Res.* (2008); 77:325–333.

Saez J.C, Retamal M.A, Basilio D., Bukauskas F.F., Bennett M.V. Connexin based gap junction hemichannels: gating mechanisms. *Biochim Biophys Acta.* (2005); 1711:215–224.

Saez J.C., Leybaert L. Hunting for connexin hemichannels. *FEBS Lett.* (2014); 588:1205–1211.

Sáeza J.C., Schalpera K.A., Retamalc M.A., Orellanaa J.A., Shojia K.F., Bennettd M.V.L. Cell membrane permeabilization via connexin hemichannels in living and dying cells. *Experimental Cell Research* (2010); 316:2377-2389.

Sakurai T., Tsuchida M., Lampe P.D., Murakami M. Cardiomyocyte FGF signaling is required for Cx43 phosphorylation and cardiac gap junction maintenance. *Exp. Cell Res.* (2013); 319: 2152–2165.

Sardão V.A., Oliveira P.J., Holy J., Oliveira C.R., Wallace K.B. Doxorubicin-induced mitochondrial dysfunction is secondary to nuclear p53 activation in H9c2 cardiomyoblasts. *Cancer Chemother. Pharmacol.* (2009); 64: 811–827

Schulte T.W., Akinaga S., Soga S., Sullivan W., Stensgard B., Toft D., Neckers L.M. Antibiotic radicicol binds to the N-terminal domain of Hsp90 and shares important biologic activities with geldanamycin. *Cell Stress Chaperones*. (1998); 3 (2): 100-8.

Schulz R., Gorge P.M., Gorbe A., Ferdinandy P., Lampe P.D., Leybaert L. Connexin 43 is an emerging therapeutic target in ischemia/reperfusion injury, cardioprotection and neuroprotection. *Pharmacol Ther*. (2015); 153:90–106.

Sellitto A.D., Al-Dadah A.S., Schuessler R.B., Nichols C.G., Lawton J.S. An open sarcolemmal adenosine triphosphate-sensitive potassium channel is necessary for detrimental myocyte swelling secondary to stress. *Circulation*. (2011); 124:S70–S74.

Severs N.J., Coppin S.R., Dupont E., Yeh H.I., Ko Y.S., Matsushita T. Gap junction alterations in human cardiac disease. *Cardiovasc Res* (2004); 62:368–77.

Severs N.J., Bruce A.F., Dupont E., Rothery S. Remodelling of gap junctions and connexin expression in diseased myocardium. *Cardiovasc Res*. (2008); 80: 9–19.

Shimizu S., Oikawa R., Tsounapi P., Inoue K., Shimizu T., Tanaka K., Martin D.T., Honda M., Sejima T., Tomita S., Saito M. Blocking of the ATP sensitive potassium channel ameliorates the ischaemia-reperfusion injury in the rat testis. *Andrology* (2014); 2: 458-465.

Shi-Yun M., Xiang-Yan M., Zhong-Wei X., Wen-Cheng Z., Xiao-Han J., Xi C., Xin Z., Yu-Ming L., Rui-Cheng X. The role of ZFP580, a novel zinc finger protein, in TGF-mediated cytoprotection against chemical hypoxia-induced apoptosis in H9c2 cardiac myocytes. *Molecular Medicine Reports*.(2017); 15: 2154-2162.

Shyng S., Nichols C.G. Octameric stoichiometry of the K_{ATP} channel complex. *J Gen Physiol.* (1997); 110:655–664.

Singal P.K., Li T., Kumar D., Danelisen I., Iliskovic N. Adriamycin-induced heart failure: Mechanism and modulation. *Mol Cell Biochem.* (2000); 207: 77-86.

Smuder A.J., Kavazis A.N., Min K., Powers S.K. Doxorubicin-induced markers of myocardial autophagic signaling in sedentary and exercise trained animals. *J Appl Physiol.* (2013); 115:176–85.

Smyth J.W., Zhang S.S., Sanchez J.M., Lamouille S., Vogan J.M., Hesketh G.G., Hong T., Tomaselli G.F., Shaw R.M. A 14-3-3 mode-1 binding motif initiates gap junction internalization during acute cardiac ischemia. *Traffic.* (2014); 15:684–699.

Solan J.L., Lampe P.D. Connexin phosphorylation as a regulatory event linked to gap junction channel assembly. *Biochimica et Biophysica Acta* (2005); *Biomembranes*. 1711(2):154–163.

Solan J.L., Lampe P.D. Connexin43 phosphorylation: Structural changes and biological effects. *Biochem. J.* (2009); 419: 261–272.

Srisakuldee W., Jeyaraman M.M., Nickel B.E., Tanguy S., Jiang Z.S., Kardami E. Phosphorylation of connexin-43 at serine 262 promotes a cardiac injury-resistant state, *Cardiovasc Res.* (2009); 83: 672–681.

Srisakuldee W., Makazan Z., Nickel B.E., Zhang F., Thliveris J.A., Pasumarthi K.B., Kardami E. The FGF-2-triggered protection of cardiac subsarcolemmal mitochondria from calcium overload is mitochondrial connexin 43-dependent. *Cardiovasc Res.*(2014); 103(1):72-80.

Takemura G., Fujiwara H. Doxorubicin-induced cardiomyopathy from the cardiotoxic mechanisms to management. *Prog. Cardiovasc. Dis.* (2007); 49: 330–352.

Toko H., Oka T., Zou Y., Sakamoto M., Mizukami M., Sano M. Angiotensin II type 1a receptor mediates doxorubicin-induced cardiomyopathy. *Hypert Res.* (2002); 25:597–603.

Von Hoff D.D., Layard M.W., Basa P., et al. Risk factors for doxorubicin-induced congestive heart failure. *Ann Intern Med.* (1979); 91:710-7.

Van Veen A.A., van Rijen H.V., Opthof T. Cardiac gap junction channels: modulation of expression and channel properties. *Cardiovasc Res.* (2001); 51: 217-29.

Wallace K.B. Doxorubicin-induced cardiac mitochondrionopathy. *Pharmacol. Toxicol.* (2003); 93: 105–115.

Wang N., De Bock M., Antoons G., Gadicherla A.K., Bol M., Decrock E., Evans WH, Sipido KR, Bukauskas FF, Leybaert L. Connexin mimetic peptides inhibit Cx43 hemichannel opening triggered by voltage and intracellular Ca^{2+} elevation. *Basic Res Cardiol.* (2012a); 107:304.

Wang N., De Bock M., Decrock E., Bol M., Gadicherla A., Bultynck G., Leybaert L. Connexin targeting peptides as inhibitors of voltage- and intracellular Ca^{2+} -triggered Cx43 hemichannel opening. *Neuropharmacology.* (2013 a); 75:506–516.

Wang N., De Vuyst E., Ponsaerts R., Boengler K., Palacios-Prado N., Wauman J., Lai C.P., De Bock M., Decrock E., Bol M., Vinken M., Rogiers V., Tavernier J., Evans W.H., Naus C.C., Bukauskas F.F., Sipido K.R., Heusch G., Schulz R., Bultynck G., Leybaert L. Selective inhibition of Cx43 hemichannels by Gap19 and its impact on myocardial ischemia/reperfusion injury. *Basic Res Cardiol.* (2013 b); 108:309.

Wang Z., Liao S.G., He Y., Li, J., Zhong R.F., He X., Liu Y., Xiao T.T., Lan Y.Y., Long Q.D., Wang Y.L. Protective effects of fractions from *Pseudostellaria heterophylla* against cobalt chloride-induced hypoxic injury in H9c2 cell. *J Ethnopharmacol.* (2013); 147(2):540-5.

Waza AA., Andrabi K., Hussain MU. Protein kinase C (PKC) mediated interaction between connexin43 (Cx43) and K⁽⁺⁾(ATP) channel subunit (Kir6.1) in cardiomyocyte mitochondria: Implications in cytoprotection against hypoxia induced cell apoptosis. *Cell. Signal.* (2014); 26: 1909–1917.

Wei C., Li H., Han L., Zhang L., Yang X. Activation of autophagy in ischemic postconditioning contributes to cardioprotective effects against ischemia/reperfusion injury in rat hearts. *J Cardiovasc Pharmacol.* (2013); 61: 416-422.

Wided K., Hassiba R., Mesbah L. Polyphenolic fraction of Algerian propolis reverses doxorubicin induced oxidative stress in liver cells and mitochondria. *Pak. J. Pharm. Sci.* (2014); 27: 1891–1897.

Willecke K., Eiberger J., Degen J., Eckardt D., Romualdi A., Guldenagel M., Deutsch U., Sohl G. Structural and functional diversity of connexin genes in the mouse and human genome. *Biol Chem.* (2002); 383:725–737.

Wong J. Smith L.B., Magun E.A., Engstrom T., Kelley-Howard K., Jandhyala D.M., Thorpe C.M., Magun B.E., Wood L.J. Small molecule kinase inhibitors block the ZAK-dependent inflammatory effects of doxorubicin. *Cancer Biol Ther.* (2013); 14: 56–63.

Wu Z., Zhang J., Zhao B. Superoxide anion regulates the mitochondrial free Ca^{2+} through uncoupling proteins. *Antioxid. Redox Signal.* (2009); 11: 1805–1818.

Wu X., Huang W., Luo G. Hypoxia induces connexin 43 dysregulation by modulating matrix metalloproteinases via MAPK signaling. *Mol. Cell. Biochem.* (2013); 384:155-162.

Xujie L., Xinggang W., Xian Z., Yeqing X., Ruizhen C., Haozhu C. C57BL/6 Mice are More Appropriate than BALB/C Mice in Inducing Dilated Cardiomyopathy with Short-Term Doxorubicin Treatment. *Acta Cardiol. Sin.* (2012); 28: 236–240.

Young J.C., Hoogenraad N.J., Hartl F.U. Molecular chaperones Hsp90 and Hsp70 deliver preproteins to the mitochondrial import receptor Tom70. *Cell*. (2003); 112: 41–50

Zhang Y., Shi J., Li Y. J., Wei L. Cardiomyocyte death in doxorubicin-induced cardiotoxicity. *Arch Immunol Ther Exp (Warsz)* (2009); 57: 435–445.

Zhang H., Flagg T.P., Nichols C.G. Cardiac sarcolemmal K(ATP) channels: latest twists in a questing tale! *J Mol Cell Cardiol*. (2010); 48:71–5.

Zhang S., Liu X., Bawa-Khalfe T, Lu L.S., Lyu Y.L., Liu L.F., Yeh E.T. Identification of the molecular basis of doxorubicin-induced cardiotoxicity. *Nat. Med.* (2012); 18:1639-42.

Zhang Y., Chen Y., Zhang M., Tang Y., Xie Y., Huang X., Li Y. Doxorubicin induces sarcoplasmic reticulum calcium regulation dysfunction via the decrease of SERCA2 and phospholamban expressions in rats. *Cell Biochem. Biophys*. (2014); 70: 1791–1798.

PUBLICATIONS

Popolo A, **Pecoraro M**, Pinto A. Effect of adenosine on isoproterenol-induced hypertrophy in vitro. A preliminary study. *PhOL, Sections Archives*, Vol.1, pp 121-126, **2014**.

Pecoraro M, Sorrentino R, Franceschelli S, Del Pizzo M, Pinto A, Popolo A. Doxorubicin-Mediated Cardiotoxicity: Role of Mitochondrial Connexin 43. *Cardiovasc Toxicol*. **2015**

Pecoraro M, Verrilli V, Pinto A, Popolo A. Role of connexin 43 in cardiovascular diseases. *Eur J Pharmacol*. **2015**. pii: S0014-2999(15)30311-3.

Sorrentino R, Terlizzi M, Di Crescenzo VG, Popolo A, **Pecoraro M**, Perillo G, Galderisi A, Pinto A. Human Lung Cancer-Derived Immunosuppressive Plasmacytoid Dendritic Cells Release IL-1 α in an AIM2 Inflammasome-Dependent Manner. *Am J Pathol*. **2015**; 185(11):3115-24.

Pecoraro M, Del Pizzo M, Marzocco S, Sorrentino R, Ciccarelli M, Iaccarino G, Pinto A, Popolo A. Inflammatory mediators in a short-time mouse model of doxorubicin-induced cardiotoxicity. *Toxicol Appl Pharmacol*. **2016**; 293:44-52.

Saturnino C, Popolo A, Ramunno A, Adesso S, **Pecoraro M**, Plutino MR, Rizzato S, Albinati A, Marzocco S, Sala M, Iacopetta D, Sinicropi MS. Anti-Inflammatory, Antioxidant and Crystallographic Studies of N-Palmitoyl-ethanol Amine (PEA) Derivatives. *Molecules*. **2017**;22(4). pii: E616.

Alburquerque-Béjar J; Barba, I.; Valls-Lacalle, L; RuizMeana, Marisol; **Pecoraro, M**; Rodríguez-Sinovas, A; García-Dorado, D. Remote ischemic conditioning provides humoral crossspecies cardioprotection through glycine receptor activation. *Cardiovasc Res*. **2017**;113(1):52-60.

Pecoraro M; Rodríguez-Sinovas A; Marzocco S; Ciccarelli M; Iaccarino G; Pinto A; Popolo A. Cardiotoxic Effects of Short-Term Doxorubicin Administration: Involvement of Connexin 43 in Calcium Impairment. *Int. J. Mol. Sci*. **2017**, 18(10), 2121.

Pecoraro M, Pinto A, Popolo A. Inhibition of Connexin 43 translocation on mitochondria accelerates CoCl₂-induced apoptotic response in a chemical model of hypoxia. *Toxicol In Vitro*. **2017**. pii: S0887-2333(17)30354-5.

De Falco G; Colarusso C; Terlizzi M; Popolo A; **Pecoraro M**; Commodo M; Minutolo P; Sirignano M; D'Anna A; Aquino RP, Pinto A; Molino A; Sorrentino R. Chronic obstructive pulmonary disease (COPD)-derived circulating cells release IL-18 and IL-33 under ultrafine particulate (UFP) matter exposure in a caspase-1/8-independent manner. Original Research, Front. Immunol. – Inflammation. **2017** 26;8:1415.

Pecoraro M; Ciccarelli M; Fiordelisi A; Iaccarino G; Pinto A; Popolo A. Diazoxide Improves Mitochondrial Connexin 43 Expression in a Mouse Model of Doxorubicin-Induced Cardiotoxicity. Int. J. Mol. Sci. **2018**. 7;19(3). pii: E757